Available online at www.sciencedirect.com

ScienceDirect

Biochimie Open 1 (2015) 11–27

www.elsevier.com/locate/biopen

Palmitoyl-ceramide accumulation with necrotic cell death in A549 cells, followed by a steep increase in sphinganine content

Mototeru Yamane*

Department of Biochemistry, Tokyo Medical University, 6-1-1 Shinjuku, Shinjuku-ku, Tokyo 160-0023, Japan

Received 11 May 2015; accepted 3 June 2015
Available online 21 June 2015

Abstract

Ceramides (Cers) have recently been identified as key signaling molecules that mediate biological functions such as cell growth, differentiation, senescence, apoptosis, and autophagy. However, the functions of Cer accumulation in necrotic cell death remain unknown. The aim of this study was to clarify the relationship between Cer accumulation with inhibition of the conversion pathway of Cer and concomitant necrotic cell death. In order to minimize the effect of apoptosis against necrotic cell death, A549 cells having the inhibiting effect of caspase 9 by survivin were used in this study. Consequently, Cer accumulation in A549 cells would likely be associated with a pathway other than the mitochondrial caspase-dependent pathway of apoptosis. Here, we showed that the dual addition of a glucosyl-Cer synthase inhibitor and a ceramidase inhibitor to A549 cell culture induced palmitoyl-Cer accumulation with Cer synthase 5 expression and necrotic cell death with lysosomal rupture together with leakage of cathepsin B/alkalization after 2–3 h, although it is unknown in this study whether the necrotic cell death was caused by the lysosomal rupture. This Cer accumulation was followed by a steep increase in sphinganine base levels via the activation of serine palmitoyltransferase activity brought about by the increase in palmitoyl-coenzyme A concentration as a substrate after 5–6 h. The increase in palmitoyl-coenzyme A concentration was achieved by activation of the fatty acid synthetic pathway from acetyl coenzyme A.

Keywords: Sphinganine; Palmitoyl-ceramide; Necrosis; DL-PDMP; D-NMAPPD; A549 cells.

1. Introduction

Ceramides (Cers) have recently been identified as key signaling molecules that mediate biological functions such as cell growth, differentiation, senescence, apoptosis, and autophagy. Cers, the central molecule involved in sphingolipid biosynthesis, can be generated through the action of ceramide

Abbreviations used: Cer, ceramide; CerS, ceramide synthase; SPT, serine palmitoyltransferase; C16:0-Cer, palmitoyl-ceramide; d18:0, sphinganine; d18:1, sphingosine; Ser, Serine; GlcCer, glucosylceramide; SM, sphingomyelin; DL-PDMP, DL-threo-1-phenyl-2-decanoylamino-3-morpholino-1-propanol; D-NMAPPD, N-[(1R,2R)-2-hydroxy-1-(hydroxy-methyl)-2-(4-nitrophenyl)ethyl]tetradecanamide; C16:0-CoA, palmitoyl-coenzyme A; C2:0-CoA, acetyl-coenzyme A; [D_7]d18:0, D-erythro-sphinganine-D7; [D_7]d18:1, D-erythro-sphingosine-D7; d18:1-[D_{31}]C16:0-Cer, N-palmitoyl [D_{31}]-D-erythro-sphingosine; IS, internal standard; L-[2,3,3-D_3]Ser, L-serine-2,3,3-D_3 ; [1,2,3,4-$^{13}C_4$]C16:0 acid, palmitic acid-1,2,3,4-$^{13}C_4$; [2-^{13}C]C2:0 acid, sodium acetate-2-^{13}C; ([$^{13}C_{16}$]C16:0-CoA, palmitoyl-$^{13}C_{16}$ coenzyme A; acridine orange, 3,6-Bis(dimethylamino) acridine hydrochloride; Myriocin, 2-amino-3,4-dihydroxy-2-(hydroxymethyl)-14-oxo-6-eicosenoic acid; SPTLC, SPT-long chain base subunit; DMEM, Dulbecco's modified Eagle's medium; FBS, fetal bovine serum; BSA, bovine serum albumin; APCI, atmospheric pressure chemical ionization; ESI, electrospray ionization; MAM, mitochondria-associated membrane; SIM, selected-ion monitoring; LDH, lactate dehydrogenase; DMSO, dimethylsulfoxide; DAPI, 4′,6-diamidino-2-phenylindole; DTT, dithiothreitol; SDS, sodium dodecyl sulfate; SDS-PAGE, sodium dodecyl sulfate-polyacrylamide gel electrophoresis; LMP, lysosomal membrane permeabilization; FATP1, fatty acid transport protein 1; 4-HPR, N-(4-hydroxyphenyl)retinamide; CHOP, CAAT/enhancer binding protein homologous protein; LC3, microtubule-associated protein 1 light chain 3B; CathB, cathepsin B; Lys, lysosomes; ER, endoplasmic reticulum.

* Fax: +81 3 3739 9945.
E-mail address: m-yamane@tokyo-med.ac.jp, CBC01664@nifty.com.

http://dx.doi.org/10.1016/j.biopen.2015.06.001

synthases (CerS) in the *de novo* synthesis pathway via serine palmitoyltransferase (SPT) or the salvage pathway. Six different CerS (CerS1 – 6) have been described, each utilizing fatty acyl CoAs of relatively defined chain lengths for N-acylation of sphingoid long chain base [sphinganine (d18:0) and sphingosine (d18:1)]. CerS1 synthesizes mostly C18:0-/C18:1-Cer, CerS2 synthesizes preferentially C22:0-/C24:0-/C24:1-Cer, CerS3 synthesizes very long chain Cers (>C26:0-Cer), CerS4 synthesizes mostly C18:0-/C20:0-/C24:0-Cer, and CerS5/6 synthesizes mainly C14:0-/C16:0-Cer [1].

In recent years, the formation of Cer channel via the interaction with Bax in the mitochondrial outer membrane, followed by the release of cytochrome c into the cytoplasm for the activation of the mitochondrial pathway of apoptosis and a direct Cer-autophagosomal membrane interaction for mitophagy have been reported [2,3]. However, the functions of Cer accumulation in necrotic cell death remain unknown. The aim of this study was to clarify the relationship between Cer accumulation with inhibition of the conversion pathway of Cer and concomitant necrotic cell death. In order to minimize the influence of apoptosis against necrotic cell death, A549 cells having the inhibiting effect of caspase 9 brought about by survivin were used in this study. Consequently, active caspase 3 expression with palmitoyl-Cer (C16:0-Cer) accumulation in A549 cells was not detected by the inhibiting effect of caspase 9 activation by survivin in the cells [4,5], and C16:0-Cer accumulation in A549 cells would likely be associated with a pathway other than the mitochondrial caspase-dependent pathway including the Bax/Bak activation of apoptosis. Previously, we showed that a high concentration of DL-threo-1-phenyl-2-decanoylamino-3-morpholino-1-propanol [DL-PDMP, an inhibitor of glucosyl(Glc)-Cer synthase] [6] in A549 cell culture caused massive autophagy with endoplasmic reticulum stress and C16:0-Cer accumulation via CerS5 protein expression in A549 cells, followed by autophagic cell death 24 h after treatment [5]. Here, we showed that the dual addition of DL-PDMP and N-[(1R,2R)-2-hydroxy-1-(hydroxymethyl)-2-(4-nitrophenyl)ethyl]tetradecanamide (D-NMAPPD, an inhibitor of ceramidase) [7] to A549 cell culture induced an additional C16:0-Cer accumulation with CerS5 expression and necrotic cell death with lysosomal rupture together with leakage of cathepsin B/alkalization after 2–3 h. This Cer accumulation was followed by a steep increase in d18:0 base levels via the activation of SPT activity brought about by the increase in palmitoyl-coenzyme A (C16:0-CoA) concentration as a substrate after 5–6 h.

2. Materials and methods

2.1. Materials

D-erythro-sphinganine-D_7 ([D_7]d18:0), D-erythro-sphingosine-D_7 ([D_7]d18:1), and N-palmitoyl [D_{31}]-D-erythro-sphingosine (d18:1-[D_{31}]C16:0-Cer) as internal standards (ISs) labeled with stable isotopes or 1-deoxysphinganine were obtained from Avanti Polar Lipids, Inc. (Alabaster, AL, USA). L-serine-2,3,3-D_3 (L-[2,3,3-D_3]Ser) as the tracer labeled with stable isotopes was purchased from Cambridge Isotope Laboratories, Inc. (Andover, MA, USA). Palmitic acid-1,2,3,4-$^{13}C_4$ ([1,2,3,4-$^{13}C_4$]C16:0 acid) or sodium acetate-2-^{13}C ([2-^{13}C]C2:0 acid) as the tracer labeled with stable isotopes, palmitoyl-$^{13}C_{16}$ coenzyme A ([$^{13}C_{16}$]C16:0-CoA) lithium salt as the IS, palmitoyl-coenzyme A (C16:0-CoA) lithium salt, sucrose monolaurate, pyridoxal 5′-phosphate hydrate, fumonisin B(1) and bovine albumin (essentially fatty acid free) were obtained from Sigma–Aldrich, Co. (St. Louis, MO, USA). NEFA C (kit for the measurement of free fatty acid content), 3,6-Bis(dimethylamino) acridine hydrochloride solution (acridine orange solution, 1 mg/ml water), Celite, 10% ammonia aqueous solution, sodium tetrahydroborate (sodium borohydride), dithiothreitol, and lithium dodecyl sulfate were purchased from Wako (Osaka, Japan). D-NMAPPD as an inhibitor of ceramidase and 2-amino-3,4-dihydroxy-2-(hydroxymethyl)-14-oxo-6-eicosenoic acid (myriocin) as an inhibitor of SPT were purchased from Cayman Chemical (Ann Arbor, MI, USA). DL-PDMP was obtained from Biomol Research Labs. (Plymouth Meeting, PA, USA). Anti-Cer synthase 5 (anti-LASS5) antibody (PAB8802) was procured from Abnova (Taipei, Taiwan). Anti-Cer synthase 6 (anti-LASS6) antibody (GTX51627) was procured from Genetex, Inc. (Irvine, CA, USA). Anti-SPT-long chain base subunit-1 (anti-SPTLC1) antibody and anti-SPT-long chain base subunit-2 (anti-SPTLC2) antibody were obtained from Acris Antibodies GmbH (Herford, Germany). Anti-SPT-long chain base subunit-3 (anti-SPTLC3) antibody was purchased from Santa Cruz Biotechnology, Inc. (Santa Cruz, CA, USA).

2.2. A549 cell culture, induction of Cer accumulation and tracer experiments

A549 cells (human lung adenocarcinoma cell line) were grown in humidified air with 5% CO_2 in Dulbecco's modified Eagle's medium (DMEM) (including 8.5 μM free fatty acids) prepared from Sigma D5796 including 400 μM L-Ser, containing fetal bovine serum (FBS) at the concentration of 10% (v/v), at 37 °C. The induction of Cer accumulation or tracer experiments were usually initiated 1 day after subculture below 90% confluence. Overgrown cells were unsuitable for obtaining the desired effects. In the tracer experiments, 1180 μM L-[2,3,3-D_3]Ser, 5.6 mM [2-^{13}C]C2:0 acid or bovine serum albumin (BSA) binding 2.34–130 μM [1,2,3,4-$^{13}C_4$] C16:0 acid in the culture medium was used. Binding of [1,2,3,4-$^{13}C_4$] C16:0 acid to BSA was performed following the method of Spector and Hoak [8]. Briefly, 100 μM [1,2,3,4-$^{13}C_4$] C16:0 acid in 10 ml of hexane was mixed with 1 g of Celite, and the mixture was evaporated dry under reduced pressure. Celite coated with fatty acid was mixed with 0.68 g of fatty acid-free BSA in 40 ml of Sigma D5796 medium, and the mixture was stirred for 30 min at room temperature. The mixture was centrifuged at 600× *g* for 5 min. The supernatant was filtered through a filter paper and Millex GS (Millipore, Billerica, MA, USA). The concentration of BSA binding C16:0 acid in the supernatant was measured using a NEFA C kit.

For the induction of Cer accumulation, 200 μM DL-PDMP and 65 μM D-NMAPPD in the culture medium were used. For the inhibition of SPT or CerS, 0.2 μM myriocin or 38 μM fumonisin B(1) was added to the culture medium.

2.3. Extraction and analysis of Cers, dihydro-Cers and glucosyl-ceramides (GlcCers) in A549 cells

A549 cells were collected each time by scraping with the culture medium and rinsing two times with Hank's balanced salt solution. Cells were homogenized for 30 s using a Polytron (Kinematica, Switzerland) in 2.5 ml of 50 mM Tris–HCl buffer (pH 7.5). The protein concentration of the homogenate was measured using BCA Protein Assay Reagents (Thermo Scientific). Then, 879 pmol d18:1-[D_{31}] C16:0-Cer- as the IS, 2.0 ml of methanol, 1.0 ml of water and 2.0 ml of chloroform were added to 1.0 ml of the homogenate, and the mixture was shaken for 30 s. The mixture was centrifuged at 600× *g* for 10 min. Then, the lower layer was transferred to a glass tube. The collected chloroform solution was evaporated dry under reduced pressure. Afterwards, the residue was dissolved in 0.5 ml of chloroform, and the solution was applied to a Sep-Pak Plus Silica cartridge (Waters, Milford, MA, USA) equilibrated with chloroform:carbontetrachloride (2:1). The cartridge was successively eluted with 15 ml of chloroform:carbontetrachloride (2:1) and 6.0 ml of chloroform:methanol (19:1). The eluates of chloroform:methanol (19:1) containing Cers and GlcCers were mixed, and the eluate was evaporated dry under reduced pressure. This process is required to lower the contamination of diacylglycerides with polarity and molecular weight similar to Cers from the sample. The residue was dissolved in 200 μl of chloroform:methanol (2:1) and 5 μl aliquots were examined using an HPLC- atmospheric pressure chemical ionization (APCI)-MS system.

2.4. Extraction and analysis of sphingo base (d18:0/d18:1/1-deoxysphinganine) in A549 cells or the subcellular fraction after various additions

The cytoplasmic extract including organelles except nuclei and the nuclear extract from A549 cells were fractionated using NE-PER Nuclear and Cytoplasmic Extraction Reagents (Thermo Scientific, Rockford, IL, USA). To 1.0 ml of the homogenate described above or cytoplasmic/nuclear extract, 0.1 ml of 10% ammonia aqueous solution, 1630 pmol of [D_7]d18:0 as the IS, 1620 pmol of [D_7]d18:0 as the IS and 2 ml of methanol were added. In the tracer experiment using the [2-^{13}C] C2:0 acid as a precursor, 2815 pmol of d18:0 as the IS instead of [D_7]d18:1 and [D_7]d18:0 was used. The mixture was treated with ultrasonic waves for 30 s. To the mixture, 2.0 ml of chloroform and 0.9 ml of 1% ammonia aqueous solution were added, and the mixture was shaken for 30 s. The mixture was centrifuged at 600× *g* for 10 min. The lower layer was transferred to a glass tube and evaporated dry under reduced pressure. The residue was dissolved in 0.2 ml of methanol, and 5 μl aliquots were examined using an HPLC-APCI-MS system.

2.5. Extraction and analysis of C16:0-CoA contents in A549 cells

Extraction and analysis of C16:0-CoA was accomplished with [$^{13}C_{16}$]C16:0-CoA as the IS using the HPLC-electrospray ionization (ESI)-MS technique modified on the basis of the method of Sun et al. [9] and Blachnio-Zabielska et al. [10]. A549 cells were collected each time by scraping with the culture medium and rinsing two times with Hank's balanced salt solution. To the cells, 0.5 ml of 100 mM KH_2PO_4 (pH 4.9), 0.5 ml of acetonitrile/2-propanol/methanol (3:1:1), and 971.8 pmol of [$^{13}C_{16}$]C16:0-CoA as the IS were added. The mixture was homogenized by vortexing for 1 min and sonicated for 30 s. The protein concentration of the homogenate was measured using BCA Protein Assay Reagents after evaporation under reduced pressure of 10 μl aliquots of the homogenate. The residual homogenate was centrifuged at 16,000× *g* (4 °C) for 10 min. The supernatant was collected and the pellet was re-extracted using 0.5 ml of acetonitrile/2-propanol/methanol (3:1:1). The two supernatants were combined and dried under reduced pressure. The dry extract was re-suspended in 100 μl of methanol/water 1:1 and centrifuged at 14,000× *g* for 10 min at 4 °C. This supernatant was used for HPLC-ESI-MS.

2.6. SPT activity and kinetics

SPT activity was measured with L-[2,3,3-D_3]Ser as a substrate using the HPLC-APCI-MS technique modified on the basis of the method of Rütti et al. [11]. A549 cells were collected by scraping with the culture medium and rinsing two times with Hank's balanced salt solution. The SPT enzyme is located in the microsomes, and the microsomes in A549 cells were cross-contaminating in the heavy membrane (mitochondria-associated membrane, MAM) fraction as previously described [5]. Therefore, the MAM fraction was isolated from A549 cells [5], and the cytoplasmic/nuclear extracts from A549 cells were fractionated as described above. The homogenate of A549 cells was prepared by Polytron treatment for 30 s in 1.5 ml of 50 mM HEPES and 1 mM EDTA buffer (pH 8.0). The protein concentration of each fraction, extract or homogenate was measured using BCA Protein Assay Reagents. The homogenate, MAM fraction, cytoplasmic extract, or nuclear extract from A549 cells was incubated at 37 °C for 1 h in 1.0 ml of 50 mM HEPES-1 mM EDTA buffer (pH 8.0) containing 0.1% (w/v) sucrose monolaurate (an inhibitor of thioesterase activity), 5 mM L-[2,3,3-D_3]Ser, 50 μM C16:0-CoA and 20 μM pyridoxal 5′-phosphate. After incubation, 250 μl of 5 mg/ml sodium tetrahydroborate was added to the mixture and the mixture was reduced at room temperature for 5 min. Extraction and analysis of the resulting [D_2]d18:0 was performed as described above.

To determine the effects of the concentration of C16:0-CoA as a substrate on the kinetics of SPT activity, a decreasing amount below 50 μM C16:0-CoA to avoid a substrate inhibition effect by C16:0-CoA was mixed with 1.0 ml of 50 mM HEPES-1 mM EDTA buffer (pH 8.0) containing 0.1% (w/v) sucrose monolaurate, 5 mM L-[2,3,3-D_3]Ser, 20 μM pyridoxal 5′-phosphate and a suspension (100 μl) of the MAM fraction from A549 cells.

Incubation, reduction, extraction and HPLC-APCI-MS analysis were performed as described above.

2.7. HPLC-APCI-MS and HPLC-ESI-MS

To determine d18:0, d18:1, Cer or GlcCer content, HPLC-MS was performed using a Shimadzu (Kyoto, Japan) LCMS-2010EV mounted on an APCI probe, and a quadrupole mass spectrometer. Connected reversed-phase HPLC separation was carried out on a Pegasil-C8 column (100 × 4.6 mm i.d.; Senshu Scientific, Tokyo, Japan) with a mobile phase of 80% methanol – formic acid (10,000:1) to d18:0/d18:1 or 100% methanol to d18:1-C16:0-Cer at a flow rate of 1.0 ml/min. In the positive ion mode (APCI probe temperature: 400 °C, detector voltage: −1.5 kV), the heat block and curved desolvation line temperature were maintained at 200 °C and 250 °C, respectively, under a nebulizer gas flow rate of 2.5 l/min.

For the quantitative determination of Cers by SIM using HPLC-APCI-MS, the peak area of $MH^+ - H_2O$ [*m/z* 493 (d18:1-C14:0-Cer), m/z 521 (d18:1-C16:0-Cer), m/z 547 (d18:1-C18:1-Cer), m/z 549 (d18:1-C18:0-Cer), m/z 577 (d18:1-C20:0-Cer), m/z 605 (d18:1-C22:0-Cer), m/z 631 (d18:1-C24:1-Cer) or m/z 633 (d18:1-C24:0-Cer)] ions as the major base ions from each Cer was compared with the sum of the peak area of $MH^+/MH^+ - H_2O$ (*m/z* 569/551) ions as the major base ions from d18:1-[D_{31}]C16:0-Cer as the IS. Since the d18:1-C16:0-Cer product derived via SPT and Cer synthase from the L-[2,3,3-D_3]Ser precursor was [D_2]d18:1-C16:0-Cer as described above [12], in the tracer experiment using L-[2,3,3-D_3]Ser as a precursor, the sum of the peak area of $MH^+/MH^+ - H_2O$ (*m/z* 523/505) ions as the major base ions from [D_2]d18:1-C16:0-Cer was compared with the sum of the peak area of the major base ions from d18:1-[D_{31}]C16:0-Cer as the IS. In the tracer experiment using the [1,2,3,4-$^{13}C_4$]C16:0 acid as a precursor, the sum of the peak area of $MH^+ - H_2O/MH^+ - 2H_2O$ (*m/z* 525/507 or 529/511) ions as the major base ions from [$^{13}C_4$]d18:1-C16:0-Cer, d18:1-[$^{13}C_4$]C16:0-Cer or [$^{13}C_4$]d18:1-[$^{13}C_4$]C16:0-Cer was compared with the sum of the peak area of the major base ions from d18:1-[D_{31}]C16:0-Cer as the IS.

For the quantitative determination of dihydro-Cers by SIM using HPLC-APCI-MS, the peak area of MH^+ [m/z 512 (d18:0-C14:0-Cer), m/z 540 (d18:0-C16:0-Cer), m/z 566 (d18:0-C18:1-Cer), m/z 568 (d18:0-C18:0-Cer), m/z 597 (d18:0-C20:0-Cer), m/z 625 (d18:0-C22:0-Cer), m/z 651 (d18:0-C24:1-Cer) or m/z 653 (d18:0-C24:0-Cer)] ions as the major base ions from each dihydro-Cer was compared with the major base ions from d18:1-[D_{31}]C16:0-Cer as the IS.

For the quantitative determination of nervonic (C24:1)-GlcCer by SIM using HPLC-APCI-MS, the sum of the peak area of MH^+-180/$MH^+ - H_2O$ (*m/z* 631/793) ions as the major base ions from C24:1-GlcCer was compared with the major base ions from d18:1-[D_{31}]C16:0-Cer as the IS.

For the quantitative determination of d18:0 or 1-deoxysphinganine by selected ion monitoring (SIM) using HPLC-APCI-MS, the sum of the peak area of $MH^+/MH^+ - H_2O$ (*m/z* 302/284 or *m/z* 286/268) ions as the major base ions from d18:0 or 1-deoxysphinganine was compared with the sum of the peak area of $MH^+/MH^+ - H_2O$ (*m/z* 309/291) ions as the major base ions from [D_7]d18:0 as the IS. Since the d18:0-product derived via SPT from L-[2,3,3-D_3]Ser-precursor/substrate was [D_2]d18:0 as previously described [12], in the tracer experiment using L-[2,3,3-D_3]Ser as a precursor/substrate, the sum of the peak area of $MH^+/MH^+ - H_2O$ (*m/z* 304/286) ions as the major base ions from [D_2]d18:0 was compared with the sum of the peak area of the major base ions from [D_7]d18:0 as the IS. In the tracer experiment using [1,2,3,4-$^{13}C_4$]C16:0 acid as a precursor, the sum of the peak area of $MH^+/MH^+ - H_2O$ (*m/z* 306/288) ions as the major base ions from [$^{13}C_4$]d18:0 was compared with the sum of the peak area of the major base ions from [D_7]d18:0 as the IS. Similarly, for the quantitative determination of d18:1/[D_7]d18:1/[$^{13}C_4$]d18:1 by SIM using HPLC-APCI-MS, the sum of the peak area of *m/z* 300/282, 302/284 or 304/286 was compared with the sum of the peak area of $MH^+/MH^+ - H_2O$ (*m/z* 307/289) ions as the major base ions from [D_7]d18:1 as the IS. In the tracer experiment using [2-^{13}C]C2:0 acid as a precursor, the variation in the incorporation of ^{13}C into d18:0 via the C16:0 acid synthetic pathway in A549 cells 6 h after various additions of [2-^{13}C]C2:0 acid was determined by SIM using HPLC-APCI-MS. Each sum of the peak area of MH^+/MH^+-H_2O (*m/z* 303–310/285–292) ions as the major base ions from [$^{13}C_{1-8}$] d18:0 was compared with the sum of the peak area of MH^+/MH^+-H_2O (*m/z* 302/284) ions as the major base ions from d18:0 as the IS or carrier.

For the quantitative determination of d18:1 or 1-deoxysphinganine by SIM using HPLC-APCI-MS, the sum of the peak area of MH^+/MH^+-H_2O (m/z 300/282 or 286/268) ions as the major base ions from d18:1 or 1-deoxysphinganine was compared with the sum of the peak area of MH^+/MH^+-H_2O (m/z 307/289) ions as the major base ions from d18:1-d_7 as the IS.

To determine C16:0-CoA contents, HPLC-MS was performed using a Shimadzu LCMS-2010EV mounted on an ESI probe. Connected RP HPLC separation was carried out on a Zorbax Extend-C18 column (150 × 2.1 mm i.d., 5 μM; Agilent Technologies, Palo Alto, CA, USA) with a mobile phase of a 0.05% triethylamine in 35% (v/v) acetonitrile at a flow rate of 0.3 ml/min. MS was performed in the negative ion mode (ESI probe temperature: 400 °C, detector voltage: −1.5 kV), and the heat block/curved desolvation line temperatures were maintained at 200 °C and 250 °C, respectively, under a nebulizer gas flow rate of 1.5 l/min. In negative ion ESI scan mass spectra of C16:0-CoA or [$^{13}C_{16}$]C16:0-CoA standards, the major fragment ion at *m/z* 501.8 from C16:0-CoA or m/z 509.8 from C16:0-$^{13}C_{16}$-CoA as the IS was the most dominant peak over the molecular ion $[M-H]^-$ at *m/z* 1004.4 from C16:0-CoA or *m/z* 1020.4 from [$^{13}C_{16}$]C16:0-CoA, which means that fatty acyl-CoA has a tendency to lose both of its hydroxyl group protons under this condition. The major fragment ions could be used as the selected ions to measure the fatty acyl-CoA concentration, as described previously [9]. For the quantitative determination of C16:0-CoA by SIM using HPLC-ESI-MS, the peak area of

m/z 501.8 ion from C16:0-CoA was compared with the peak area of *m/z* 509.8 ion from [$^{13}C_{16}$]C16:0-CoA as the IS.

2.8. Lactate dehydrogenase (LDH) release

To precisely characterize the extent of cell death, cytotoxicity was quantified by measuring [13] the activity of LDH released into the culture medium.

2.9. Morphologic assessment of cells undergoing necrotic cell death and apoptosis

A549 cells were grown in DMEM medium using BD Falcon culture slides with 4 chambers (Bedford, MA, USA). For the induction of Cer accumulation, each chamber was filled with 1.0 ml of DMEM medium containing 3 μl of dimethylsulfoxide (DMSO) as a control, 1.0 ml of DMEM medium containing 65 μM D-NMAPPD (with 3 μl of DMSO as a solvent of D-NMAPPD) as an inhibitor of ceramidase, 1.0 ml of DMEM medium containing 200 μM DL-PDMP (with 3 μl of DMSO) as an inhibitor of Glc-Cer synthase or 1.0 ml of DMEM medium containing 65 μM D-NMAPPD plus 200 μM (with 3 μl of DMSO as a solvent of D-NMAPPD) as a dual inhibitor of ceramidase and Glc-Cer synthase. Cells were incubated for 3, 4 or 6 h, and the adherent cells were washed twice with PBS(-) and stained using the GFP-Certified Apoptosis/Necrosis Detection kit (Enzo Life Sciences, Inc., Farmingdale, NY, USA) plus VECTASHIELD mounting medium with 4′,6-diamidino-2-phenylindole (DAPI, blue fluorescence) to stain the nucleus (Vector Laboratories, Inc., Burlingame, CA, USA). The morphology of the Apoptosis/Necrosis Detection kit-stained A549 cells was examined by confocal laser scanning microscopy using a ZEISS LSM-700 (Carl Zeiss Microscopy GmbH, Jena, Germany). With the Apoptosis/Necrosis Detection kit, early apoptotic cells are stained positive with the apoptosis detection reagent (Annexin V-EnzoGold, Ex/Em: 550/570 nm, yellow fluorescence) but negative with the necrotic detection reagent. On the other hand, early necrotic cells are stained positive with the necrotic detection reagent (7-AAD, Ex/Em: 546/647 nm, red fluorescence) but negative with the apoptosis detection reagent. However, late-stage apoptotic/necrotic cells are stained positive with both the apoptosis detection reagent and the necrosis detection reagent.

2.10. Lysosomal stability assay

A549 cells were grown and derivated using BD Falcon culture slides with 4 chambers as described above. After the cells were incubated for 2–4 h, acridine orange was added to a final concentration of 6.6 μM. After the cells were incubated for 45 min, the adherent cells were washed three times with PBS(-). The morphology of acridine orange-stained A549 cells was examined by confocal laser scanning microscopy using a ZEISS LSM-700. Acridine orange in active lysosomes with an acidic pH exhibited red fluorescence. On the other hand, acridine orange in the cytoplasm or nucleus with a basic pH exhibited green fluorescence. At the previous stage of plasma membrane disruption, rupture of acridine orange-loaded lysosomes may be monitored as an increase in cytoplasmic diffuse green fluorescence or a decrease in granular red fluorescence [14].

To measure cathepsin B activity in the cytosol and organelle in A549 cells, cells were treated as described above and fractionated using the Fraction PREP Cell Fractionation kit (BioVision, CA95035, USA). The cytosolic fraction was fractionated using Cytosol Extraction Buffer containing dithiothreitol (DTT), and the pellet (organelle fraction) resulting from this fractionation was collected. For the liberation of cathepsin B from the organelle fraction, the pellet was treated with ultrasonic waves for 20 s in 0.85% NaCl, and the homogenate was fractionated by centrifugation at 700× *g* for 10 min. Cathepsin B activity was measured in both the cytosolic fraction and the organelle fraction using the Cathepsin B Activity Fluorometric Assay kit (BioVision).

2.11. Western blotting with anti-Cer synthase 5/6 (CerS5/6) antibodies and anti-SPTLC1/2/3 antibodies

A549 cells were collected each time by scraping with the culture medium and rinsing two times with Hank's balanced salt solution. Since C16:0-Cer was preferentially generated by Cer synthase 5/6 [5], the detection of CerS5/6 protein in A549 cells was performed by Western blotting. The cells in 1.0 ml of 0.85% sodium chloride were mixed with 100 μl of 100% (1.0 g/ml aqueous solution) trichloroacetic acid solution and left for 30 min at 0 °C. The mixture was centrifuged at 1500× *g* for 5 min. The pellet was mixed with 80 μl of 9 M urea/2% Triton X100/1% DTT and the mixture was treated with ultrasonic waves for 30 s. The mixture was mixed with 20 μl of 10% lithium dodecyl sulfate and the mixture was made basic with 1 M Tris under ultrasonic waves for 30 s.

For the detection of SPTLC1, 2, and 3 protein, the cytoplasmic extract or nuclear extract from A549 cells was fractionated as described above, and each extract was concentrated using an ultrafiltration membrane. The protein concentration of each extract was measured using BCA Protein Assay Reagents. Each extract was mixed with an equal volume of 2× sodium dodecyl sulfate (SDS) sample buffer made up of 125 mM Tris–HCl (pH 6.8)/4% SDS/10% sucrose/2% DTT, and the mixture was heated at 95 °C for 5 min.

Samples for sodium dodecyl sulfate-polyacrylamide gel electrophoresis (SDS-PAGE) that were regulated to achieve the same expression of β-actin were loaded onto the gels and separated by 10% SDS-PAGE. After blotting and blocking, the membranes were probed with the primary antibody (anti-LASS5/6, anti-SPTLC1/2/3, or anti-β-actin). Detection was achieved using ECL-Prime Western Blotting Detection Reagent and Hyperfilm ECL (GE Healthcare, Japan).

2.12. Statistical analysis

Data were expressed as mean ± SD. To determine statistical significance, the values were compared using the two-group t-test with differences considered significant for $P < 0.05$.

3. Results

3.1. Morphology of apoptosis/necrosis detection kit-stained A549 cells after the addition of DL-PDMP, D-NMAPPD or DL-PDMP plus D-NMAPPD

The morphology of Apoptosis/Necrosis Detection kit-stained A549 cells was examined 4 h after the addition using confocal laser scanning microscopy, as shown in Fig. 1. With the dual addition of DL-PDMP and D-NMAPPD, many necrotic cells (red fluorescence, positive 7-AAD) were detected (Fig. 1D), compared with the control (Fig. 1A), D-NMAPPD-treated (Fig. 1B), or DL-PDMP-treated (Fig. 1C) cells. The ratio of apoptotic cells (yellow fluorescence, positive Annexin V-EnzoGold) to necrotic cells with the dual addition of DL-PDMP and D-NMAPPD was low (Fig. 1D). At high magnification (Fig. 1E), small numbers of typical apoptotic cells (positive yellow fluorescence and negative red fluorescence) are indicated by an arrow, although many necrotic cells showed positive strong red fluorescence and positive slight yellow fluorescence. Statistical data regarding the results obtained with the apoptosis/necrosis detection are shown in Fig. 1F. However, many necrotic cells with the triple addition of DL-PDMP plus D-NMAPPD plus myriocin were detected compared with the dual addition of DL-PDMP plus D-NMAPPD (data not shown). It was stipulated that the triple addition caused synergistical cell death by the combination of myriocin and antitumor drugs (DL-PDMP plus D-NMAPPD) against A549 cells as described previously [15].

3.2. Lysosomal stability

The time course of the liberation of cathepsin B activity from the organelle fraction is shown in Fig. 2. The dual addition of DL-PDMP and D-NMAPPD caused a significant increase in cathepsin B activity in the cytosolic fraction at the point of 2 h after the addition, compared with the control or the individual addition. It was stipulated that both Cer accumulation in lysosomes and the inhibition of lysosomal acid ceramidase by D-NMAPPD were required for the liberation of cathepsin B from lysosomes based on lysosomal membrane permeabilization (LMP), followed by lysosomal disruption and digestion of vital proteins for a lethal event, although it is unknown in this study whether the necrotic cell death was caused by the lysosomal rupture.

The morphologies of acridine orange-stained A549 cells were examined 3 h after the addition using fluorescence microscopy, as shown in Fig. 3. With the dual addition of DL-PDMP and D-NMAPPD, red fluorescence exhibiting active lysosomes with acidic pH was abolished (Fig. 3D), compared with the control (Fig. 3A), D-NMAPPD-treated (Fig. 3B), or DL-PDMP-treated (Fig. 3C) cells. Statistical data regarding the results obtained with the acridin orange staining are shown in Fig. 3E. It was stipulated that the dual addition caused an increase in the pH in acidic compartments such as lysosomes, followed by the inhibition of increased autophagosome-lysosome fusion, as described previously [14,16]. On the other hand, the addition of DL-PDMP caused an increase in red fluorescence (Fig. 3C and E), compared with the control or D-NMAPPD-treated cells. It was suggested that the addition of DL-PDMP induced the autophagosome form and the activation (an increase in red fluorescence) of lysosomal function, as described previously [5,17].

3.3. LDH release after various additions as a form of cell toxicity

The time course of LDH release (cell death) from A549 cells after the individual addition of 200 μM DL-PDMP and 65 μM D-NMAPPD or the dual addition is shown in Fig. 4. In LDH release as a form of cell toxicity such as in necrosis, the dual addition alone caused a significant increase in LDH release compared with the individual addition, in connection with the morphological changes (Figs. 1 and 3) as described above or the changes in the d18:0 contents (Fig. 6) as described below. Permeability of the cell membrane against low molecular weight-7AAD used in necrosis detection would actually be expected to be more constant over time. However, high molecular weight-LDH protein would be expected to have a sharp release with the rupture of the cell membrane in necrotic cell death.

3.4. Contents of C24:1-GlcCer/d18:1/C16:0-Cer/d18:0 and Cer synthase 5 (LASS5) protein expression in A549 cells or the subcellular fraction after various additions

C24:1-GlcCer/d18:1 contents in A549 cells after the individual addition of 200 μM DL-PDMP, 65 μM D-NMAPPD or the dual addition are shown in Fig. 5A. The addition of DL-PDMP and the dual addition caused a significant decrease in C24:1-GlcCer contents compared with the control system 6 h after the addition. Similarly, the addition of D-NMAPPD and the dual addition caused a significant decrease in d18:1 contents compared with the control system 2 h after the addition. The addition of DL-PDMP or D-NMAPPD as an inhibitor caused a decrease in the content of d18:1-C24:1-GlcCer or d18:1 as the reaction product in A549 cells.

The time course of C16:0-Cer contents in A549 cells after the individual addition of 200 μM DL-PDMP, 65 μM D-NMAPPD or the dual addition is shown in Fig. 5B. Although the individual addition of DL-PDMP or D-NMAPPD caused a time-dependent increase in C16:0-Cer contents compared with the control system from 2 to 6 h after the addition, the dual addition caused the synergistic increase in C16:0-Cer contents compared with the individual addition. The levels of Cer species including d18:1-C16:0-Cer and dihydro-Cer species in A549 cells 6 h after the individual or their dual addition are shown in Fig. 5C and D. The dual addition to A549 cells did not significantly modify the contents of other Cer/dihydro-Cer species except d18:1-C16:0-Cer/d18:0-C16:0-Cer/d18:1-C14:0-Cer/d18:0-C14:0-Cer in the HPLC-APCI-MS analysis.

The CerS5/6 protein expression levels compared with the individual addition are shown in Fig. 5E. The addition of DL-PDMP greatly increased CerS5 protein expression levels as described previously [5] and the dual addition caused a synergistic increase in the CerS5 protein expression levels. However, the dual addition did not significantly modify CerS6 protein expression compared with the individual addition. It was suggested that

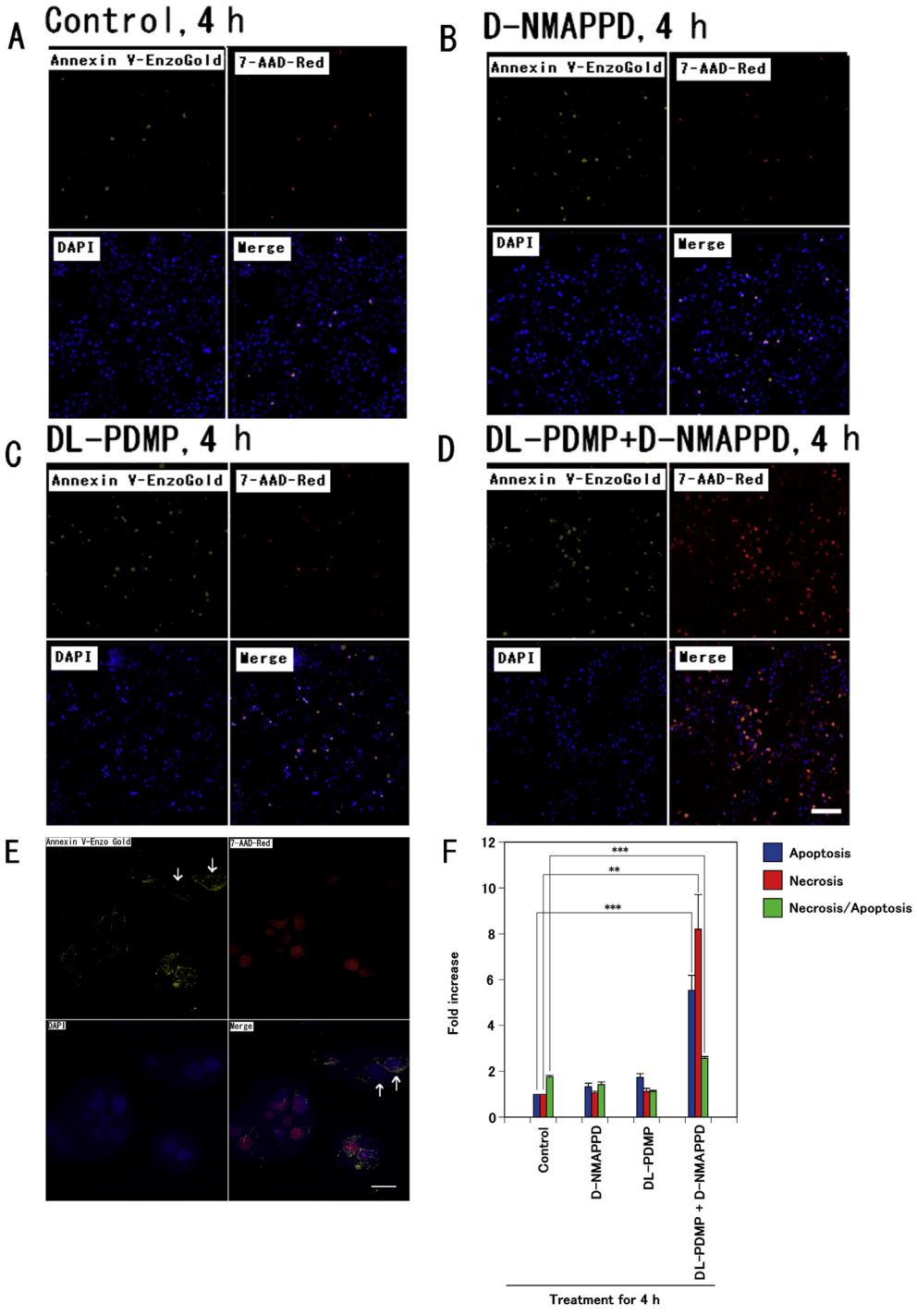

Fig. 1. The dual addition of DL-PDMP and D-NMAPPD caused necrotic A549 cell death morphologically as detected using the Apoptosis/Necrosis Detection kit. A549 cells were grown in DMEM medium using BD Falcon culture slides. The induction of Cer accumulation in BD Falcon culture slides and morphologic assessment of cells were achieved as described in the Methods. The number of nuclei in the cells stained with blue fluorescence using DAPI indicated cell density. Apoptotic cells showed yellow fluorescence staining with Annexin V-EnzoGold. Necrotic cells showed red fluorescence staining with 7-AAD. ***A***, Control (4 h). ***B***, D-NMAPPD (65 μM, 4 h). ***C***, DL-PDMP (200 μM, 4 h). ***D***, DL-PDMP (200 μM) plus D-NMAPPD (65 μM) for 4 h. ***E***, High magnification of D (DL-PDMP plus D-NMAPPD) treatment. ***F***, Statistical data regarding the results obtained with the apoptosis/necrosis detection. Data are presented as the mean values ± S.D. of three independent experiments; $^{**}P < 0.01$; $^{***}P < 0.001$ as compared with the group without the addition. Each scale bar indicates 100 μm (A–D) and 20 μm (E).

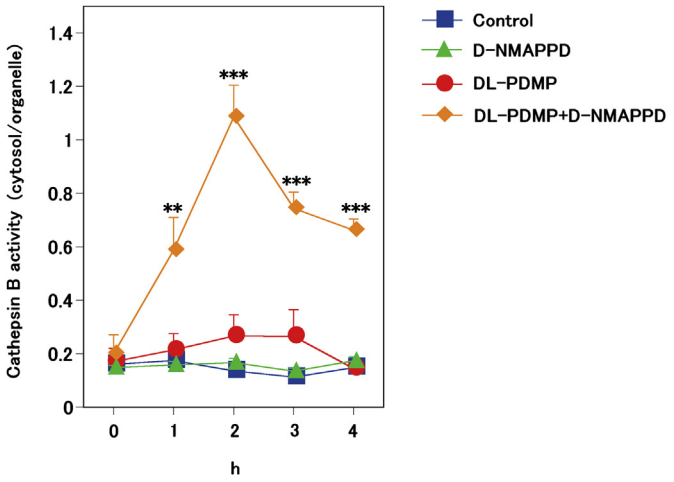

Fig. 2. The dual addition of DL-PDMP and D-NMAPPD caused a significant increase in cathepsin B activity in the cytosolic fraction at the point of 2 h after the addition. The induction of Cer accumulation and measurement of cathepsin B activity were achieved as described in the Methods. Data are presented as the mean values ± S.D. of three independent experiments; **P < 0.01; ***P < 0.001 as compared with the group without the addition.

the increase in the C16:0-Cer levels was attributable to an increase in the synthesis of C16:0-Cer based on an increase in the CerS5 protein expression by the dual addition rather than the accumulation of C16:0-Cer based on an enzyme inhibition by DL-PDMP or D-NMAPPD.

The time course of d18:0 contents in A549 cells after the individual addition of 200 μM DL-PDMP, 65 μM D-NMAPPD, or the dual addition is shown in Fig. 6. Although the individual addition of DL-PDMP or D-NMAPPD failed to increase d18:0 contents compared with the control system from 2 to 6 h after the addition, the dual addition alone caused a significant increase in d18:0 contents compared with the individual addition (Fig. 6A). It was stipulated that d18:0 production with the dual addition caused an increase (Fig. 3D) in the pH in acidic compartments such as lysosomes, followed by the inhibition of autophagosome-lysosome fusion.

The time course of d18:0 contents in the subcellular fraction of A549 cells after the dual addition is shown in Fig. 6B. The dual addition caused a significant increase in d18:0 contents from 5 to 6 h after the addition in both the cytoplasmic and nuclear fractions.

The changes in d18:0/d18:1/1-deoxysphinganine contents in A549 cells 5 h after the dual addition or the dual addition plus 38 μM fumonisin B(1) are shown in Fig. 6C. The addition of fumonisin B(1) caused a significant increase in d18:0 contents, although the addition did not significantly modify d18:1/1-deoxysphinganine contents. It was stipulated that the dual addition plus fumonisin B(1) caused the synergistic increase in d18:0 contents based on the activation of d18:0 production and the inhibition of d18:0 metabolism by fumonisin B(1).

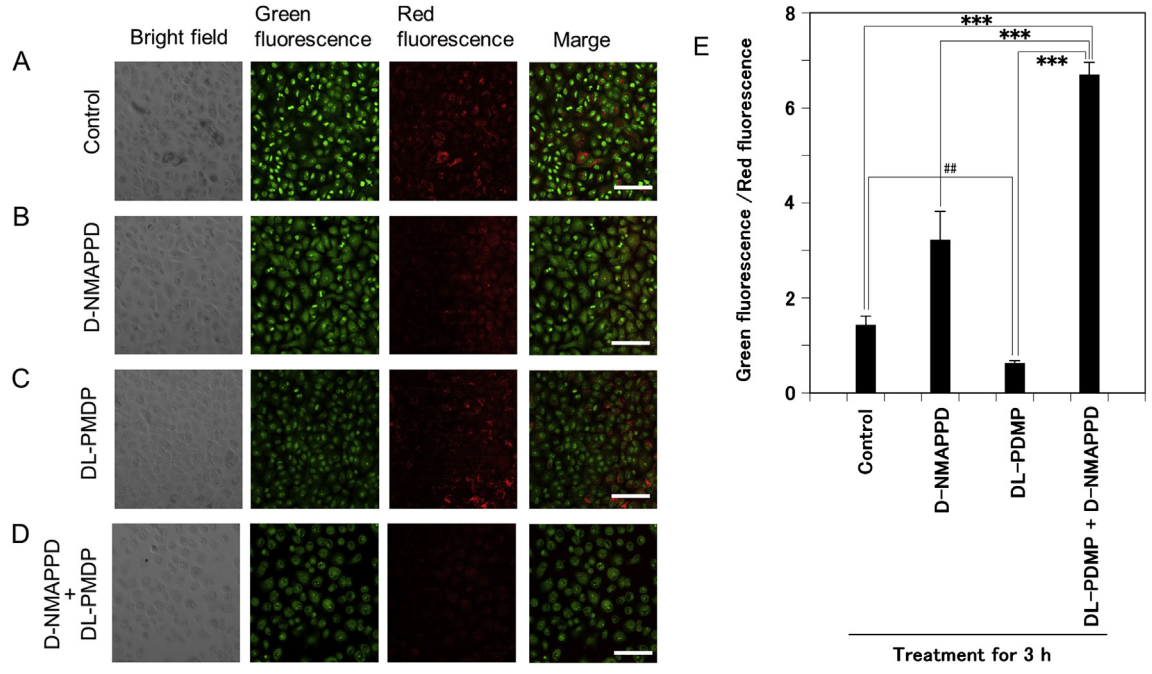

Fig. 3. The dual addition of DL-PDMP and D-NMAPPD caused an increase in pH in the cellular acidic compartments. The induction of Cer accumulation in BD Falcon culture slides and the assessment of the morphology of the acridine orange-stained A549 cells were achieved as described in the Methods. ***A***, Control (3 h). ***B***, D-NMAPPD (65 μM, 3 h). ***C***, DL-PDMP (200 μM, 3 h). ***D***, DL-PDMP (200 μM) plus D-NMAPPD (65 μM) for 3 h. In the dual addition of DL-PDMP and D-NMAPPD, red fluorescence exhibiting active lysosomes with acidic pH was abolished (***D***) compared with the control (***A***), D-NMAPPD-treated (***B***) or DL-PDMP-treated (***C***) cells. In contrast, increased green fluorescence exhibiting a basic pH was observed with the addition of DL-PDMP plus D-NMAPPD (***D***). ***E***, Statistical data regarding the results obtained with the acridin orange staining. Data are presented as the mean values ± S.D. of three independent experiments; ***P < 0.001 as compared with the group without the addition or the individual addition. ##P < 0.01 as effects with the addition of DL-PDMP. Each scale bar indicates 100 μm (A–D).

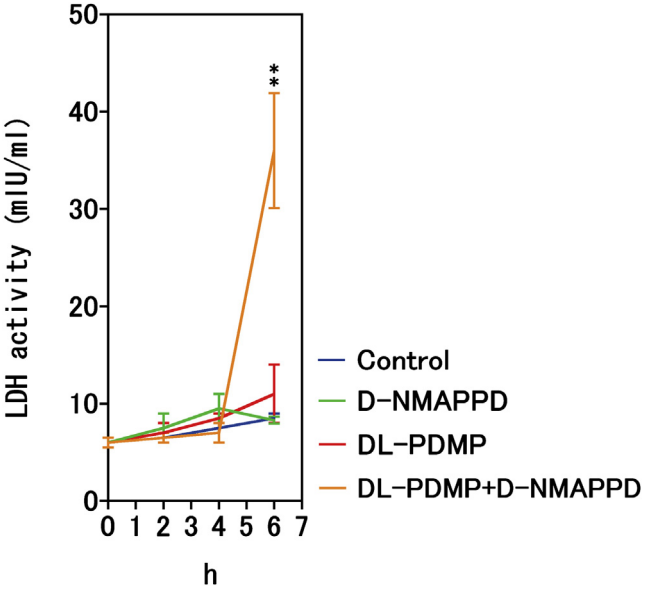

Fig. 4. The dual addition of DL-PDMP and D-NMAPPD alone caused a significant increase in LDH release (cell death) compared with the individual addition. The induction of Cer accumulation and analysis of the activity of LDH were achieved as described in the Methods. To precisely characterize the extent of cell death, cytotoxicity was quantified by measuring the activity of LDH released into the culture medium. Data are presented as the mean values ± S.D. of three independent experiments; $^{**}P < 0.01$ as compared with the group without the addition.

3.5. Tracer experiments accompanying d18:0 and C16:0-Cer accumulations in A549 cells after various additions

In the tracer experiments using L-[2,3,3-D_3]Ser, the dual addition of DL-PDMP and D-NMAPPD caused a significant increase in d18:0 and [D_2]d18:0 contents 3 or 5 h after the addition compared with the control system, as shown in Fig. 7, although the dual addition failed to increase d18:1 or [D_2]d18:1 contents. Increases in d18:0 and [D_2]d18:0 with the dual addition were inhibited by the addition of myriocin as an SPT inhibitor. It was suggested that the dual addition caused a steep increase in d18:0 contents via the incorporation of deuterium into d18:0 from L-[2,3,3-D_3]Ser, suggesting *de novo* synthesis. Furthermore, it was stipulated that the slight increase in d18:1 or [D_2]d18:1 contents was due to localized hydrolysis of an increased d18:1-C16:0-Cer contents which occurred under the inhibition of ceramidase. On the other hand, the dual addition caused a significant increase in d18:1-C16:0-Cer and [D_2]d18:1-C16:0-Cer contents 3 or 5 h after the addition compared with the control system, as shown in Fig. 8. However, although the increases in the dual addition were inhibited by the addition of myriocin, the extents of inhibition were low compared with the extents of inhibition in d18:0 and [D_2]d18:0 contents. It was stipulated that the dual addition caused the production of d18:1-C16:0-Cer via a pathway other than *de novo* synthesis, e.g., the reproduction of C16:0-Cer using C16:0-CoA and d18:1 based on an increase in the Cer synthase 5 protein expression.

In the tracer experiments using [1,2,3,4-$^{13}C_4$]C16:0 acid with the dual addition of DL-PDMP and D-NMAPPD, the variations in the incorporation of ^{13}C into d18:0 from [1,2,3,4-$^{13}C_4$]C16:0 acid are shown in Fig. 9A. It was suggested that the form of ^{13}C-incorporation into d18:0 revealed the *de novo* synthesis of d18:0,and a steep increase in d18:0 contents was caused in the optimum C16:0 acid concentration in the culture medium. The added [1,2,3,4-$^{13}C_4$]C16:0 acid will possibly be transported via fatty acid transport protein 1 (FATP1) interacted to acyl coenzyme A synthetase, as described previously [18,19]. Consequently, lowered d18:0 production with the incorporation of ^{13}C with a high concentration of C16:0 acid in the culture medium appears to be the result of substrate inhibition by C16:0-CoA as a substrate of SPT activity, as described previously [11]. On the incorporation of ^{13}C into [$^{13}C_4$]d18:1-C16:0-Cer, d18:1-[$^{13}C_4$]C16:0-Cer or [$^{13}C_4$]d18:1-[$^{13}C_4$]C16:0-Cer, it was stipulated that the dual addition caused the production of d18:1-C16:0-Cer via the double pathway of a pathway of *de novo* synthesis and a pathway other than *de novo* synthesis, e.g., the reproduction of C16:0-Cer using [$^{13}C_4$]C16:0-CoA and d18:1 based on an increase in the Cer synthase 5 protein expression (Fig. 9B).

For the quantitative determination of biosynthesized d18:0 via the C16:0 acid synthetic pathway from acetic acid, [2-^{13}C]C2:0 acid was used in the culture medium. The variations in the incorporation of ^{13}C into d18:0 in A549 cells 6 h after various additions of [2-^{13}C]C2:0 acid to the culture medium is shown in Fig. 10. The dual addition of DL-PDMP and D-NMAPPD or the addition of DL-PDMP caused a significant increase in [$^{13}C_{4-7}$]d18:0 contents compared with the control. Furthermore, the dual addition caused a significant increase in [$^{13}C_{4-7}$]d18:0 contents compared with the addition of DL-PDMP. The data from [$^{13}C_{1-3}$]d18:0 are not shown in Fig. 10 for the overlapping in *m/z* values based on the isotopic abundance ratio of d18:0 as the IS. It was suggested that the dual addition caused a significant increase in biosynthesized d18:0 contents via the C16:0 acid synthetic pathway from acetic acid compared with other additions.

3.6. C16:0-CoA accumulation in A549 cells after various additions

The changes in C16:0-CoA contents in A549 cells 5 h after various additions are shown in Fig. 11. The dual addition of DL-PDMP and D-NMAPPD or the addition of D-NMAPPD caused a significant increase in C16:0-CoA contents compared with the control in connection with morphological changes, as described above. Furthermore, the dual addition caused a significant increase in C16:0-CoA contents compared with the addition of D-NMAPPD. It was suggested that the dual addition caused a significant increase in d18:0 contents via an enhanced SPT activity with the increase in C16:0-CoA concentration as a substrate.

3.7. Kinetics of SPT activity and SPT activity in A549 cells or the subcellular fraction after various additions

SPT kinetics using the MAM fraction from A549 cells are shown in Fig. 12A. The *Km* against C16:0-CoA as a substrate was 12.5 μM. The *Vmax* was 161 pmol/mg protein/min.

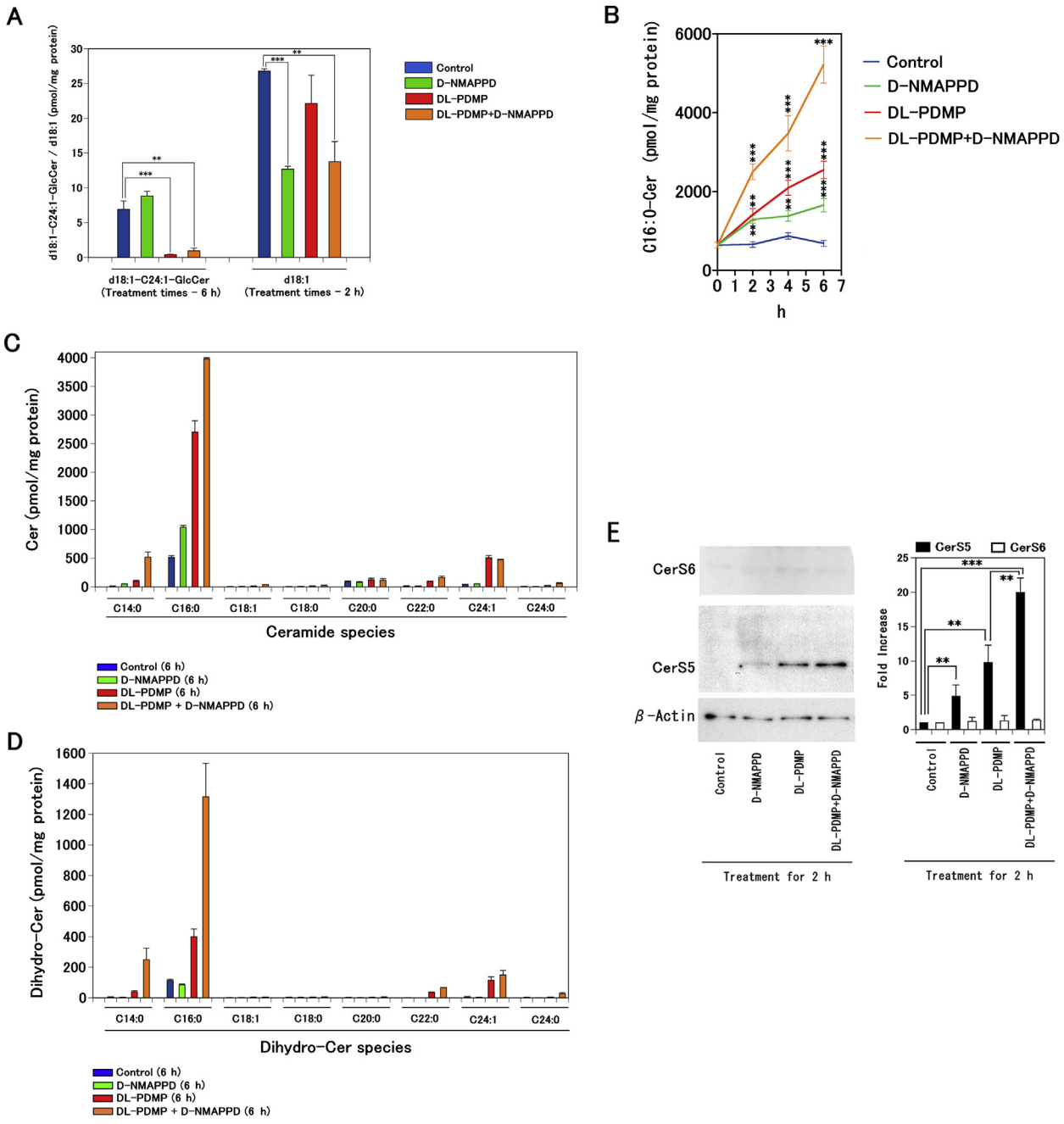

Fig. 5. The dual addition of DL-PDMP and D-NMAPPD caused an additional increase in C16:0-Cer contents with an increase in Cer synthase 5 protein expression compared with the individual addition. The induction of Cer accumulation and extraction/analysis of Cers/dihydro-Cer in the homogenate or Western blotting with anti-Cer synthase 5 antibodies were achieved as described in the Methods. ***A***, C24:1-GlcCer/d18:1 contents in A549 cells after the individual addition of 200 μM DL-PDMP, 65 μM D-NMAPPD or the dual addition. ***B***, Time course of C16:0-Cer contents in A549 cells after the individual addition of 200 μM DL-PDMP, 65 μM D-NMAPPD, or the dual addition. Data are presented as the mean values ± S.D. of three independent experiments; $^{**}P < 0.01$; $^{***}P < 0.001$ as compared with the group without the addition. ***C*** and ***D***, Levels of Cer species including d18:1-C16:0-Cer and dihydro-Cer species in A549 cells 6 h after the individual or their dual addition. The dual addition to A549 cells did not significantly modify the contents of other Cer/dihydro-Cer species except d18:1-C16:0-Cer/d18:0-C16:0-Cer/d18:1-C14:0-Cer/d18:0-C14:0-Cer in the HPLC-APCI-MS analysis. ***E***, CerS5/6 protein expression levels compared with individual addition. The addition of DL-PDMP markedly increased the CerS5 protein expression levels, as described previously [5], and the dual addition caused the synergistic increase in the CerS5 protein expression levels. Data are presented as the mean values ± S.D. of three independent experiments; $^{**}P < 0.01$; $^{***}P < 0.001$ as compared with the group without the addition.

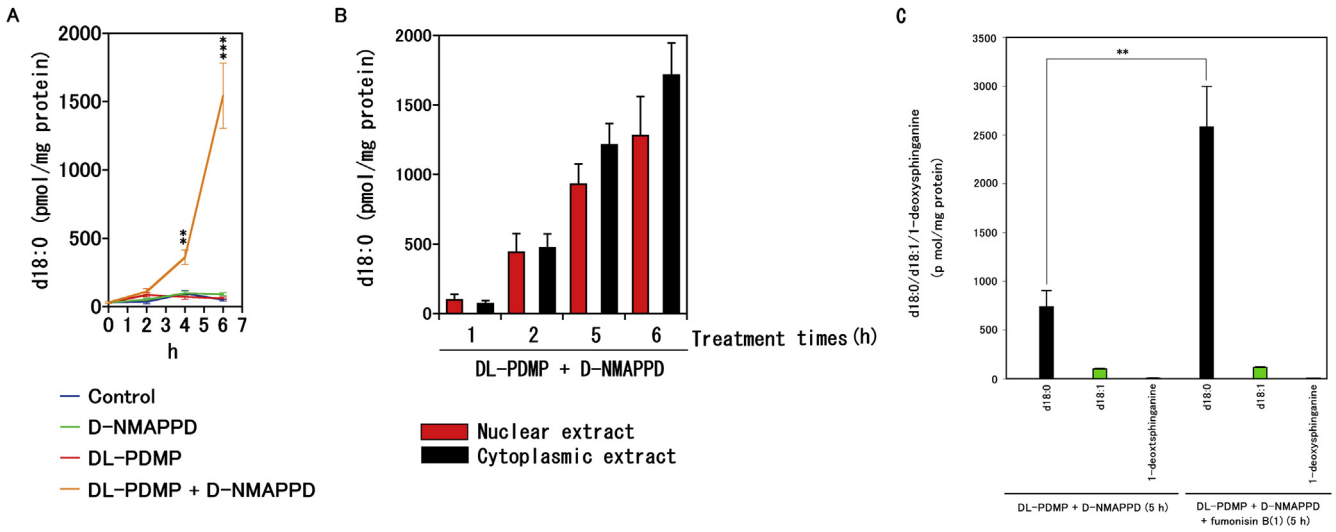

Fig. 6. The dual addition of DL-PDMP and D-NMAPPD alone caused a significant increase in d18:0 contents in the cells or subcellular fractions compared with the individual addition. The induction of Cer accumulation and extraction/analysis of d18:0/d18:1/1-deoxysphinganine in the homogenate were achieved as described in the Methods. On the other hand, the cytoplasmic extract including organelles except nuclei and the nuclear extract from A549 cells were fractionated using NE-PER Nuclear and Cytoplasmic Extraction Reagents. ***A***, Time course of d18:0 contents in A549 cells after the individual addition of 200 μM DL-PDMP and 65 μM D-NMAPPD or their dual addition. Data are presented as the mean values ± S.D. of three independent experiments; $^{**}P < 0.01$; $^{***}P < 0.001$ as compared with the group without the addition. ***B***, Time course of d18:0 contents in the subcellular fractions of A549 cells after the dual addition. Data are presented as mean values ± S.D. ***C***, Changes in d18:0/d18:1/1-deoxysphinganine contents in A549 cells 5 h after the dual addition or the dual addition plus fumonisin B(1). The addition of fumonisin B(1) caused a significant increase in d18:0 contents, although the addition did not significantly modify d18:1/1-deoxysphinganine contents. Data are presented as the mean values ± S.D. of three independent experiments; $^{**}P < 0.01$ as compared with the group without the addition of fumonisin B(1).

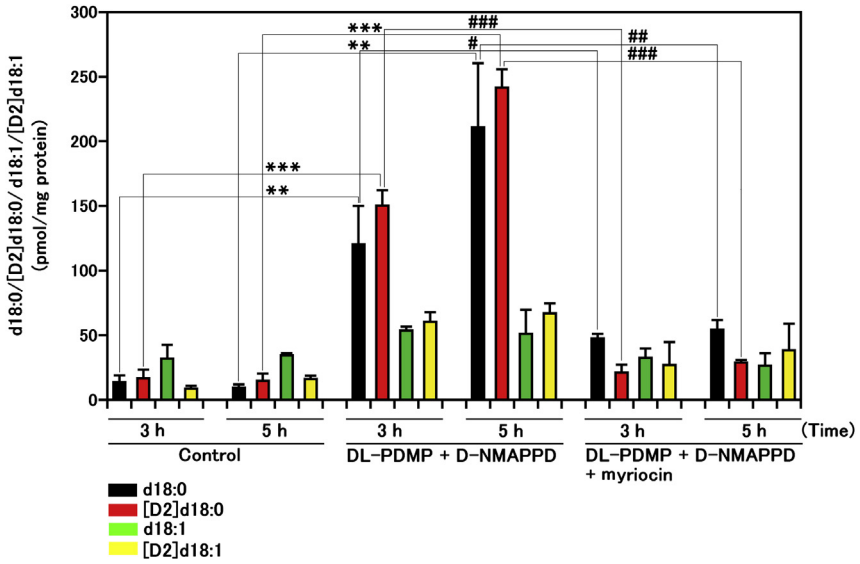

Fig. 7. In the tracer experiments using L-[2,3,3-D_3]Ser, the dual addition of DL-PDMP and D-NMAPPD caused a significant increase in d18:0 and [D_2]d18:0 contents. In the tracer experiments, 1180 μM L-[2,3,3-D_3]Ser in the culture medium was used. The induction of Cer accumulation and extraction/analysis of d18:0 in the homogenate were achieved as described in the Methods. The dual addition failed to increase d18:1 or [D_2]d18:1 contents. Increases in the d18:0 and [D_2]d18:0 contents in the dual addition were inhibited by the addition of myriocin as an inhibitor of SPT. Data are presented as the mean values ± S.D. of three independent experiments; $^{**}P < 0.01$; $^{***}P < 0.001$ as compared with the group without the addition. #, ##, and ### indicate $P < 0.05$, $P < 0.01$, and $P < 0.001$, respectively, as effects with the addition of myriocin.

The SPT activities in the homogenate from A549 cells with various additions are shown in Fig. 12B. The various additions to A549 cells did not significantly modify SPT activity in the homogenate. Furthermore, the dual addition of 200 μM DL-PDMP and 65 μM D-NMAPPD to A549 cells did not significantly or time-dependently modify SPT activity in the cytoplasmic or nuclear extract from A549 cells, as shown in Fig. 12C. It was suggested that the steep increase in d18:0 *de novo* synthesis by the dual addition was attributable to factors such as the substrate concentration other than SPT enzyme concentration.

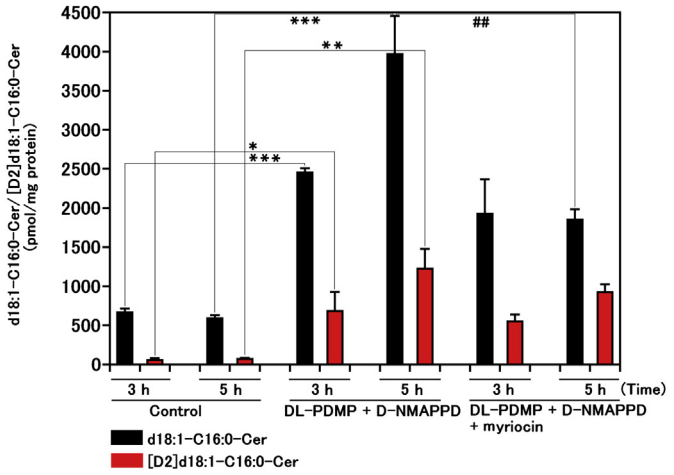

Fig. 8. In the tracer experiments using L-[2,3,3-D_3]Ser, the dual addition of DL-PDMP and D-NMAPPD caused a significant increase in d18:1-C16:0-Cer and [D_2]d18:1-C16:0-Cer contents. In the tracer experiments, 1180 μM L-[2,3,3-D_3]Ser in the culture medium was used. The induction of Cer accumulation and extraction/analysis of Cers in the homogenate were achieved as described in the Methods. The increases in the dual addition were inhibited by the addition of myriocin, and the extent of inhibition was low compared with the extent of the inhibition of the d18:0 and [D_2] d18:0-contents. Data are presented as the mean values ± S.D. of three independent experiments; *P < 0.05; **P < 0.01; ***P < 0.001 as compared with the group without the addition. ## indicates P < 0.01 as effects with the addition of myriocin.

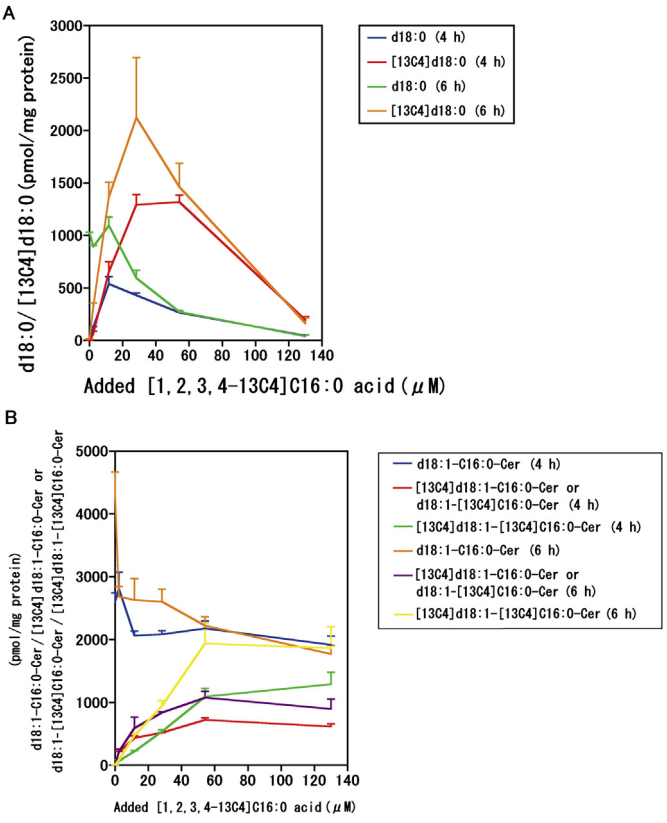

Fig. 9. In the tracer experiments using [1,2,3,4-$^{13}C_4$]C16:0 acid under the dual addition of DL-PDMP and D-NMAPPD, the variation in the incorporation of ^{13}C into d18:0 from [1,2,3,4-$^{13}C_4$]C16:0 acid revealed a form suggesting the optimum C16:0 acid concentration in the culture medium. In the tracer experiments, BSA binding 2.34–130 μM [1,2,3,4-$^{13}C_4$]C16:0 acid in the culture medium was used. The induction of Cer accumulation and extraction/analysis of d18:0 or C16:0-Cer in the homogenate were achieved as described in the Methods. ***A***, Variation in the incorporation of ^{13}C into d18:0 from [1,2,3,4-$^{13}C_4$]C16:0 acid against the additional [1,2,3,4-$^{13}C_4$]C16:0 acid. ***B***, Variation in the incorporation of ^{13}C into [$^{13}C_4$]d18:1-C16:0-Cer, d18:1-[$^{13}C_4$]C16:0-Cer or [$^{13}C_4$]d18:1-[$^{13}C_4$]C16:0-Cer from [1,2,3,4-$^{13}C_4$]C16:0 acid against the additional [1,2,3,4-$^{13}C_4$]C16:0 acid. Data are presented as the mean values ± S.D. of three independent experiments.

3.8. SPTLC1, 2, and 3 protein expression using Western blotting in cytoplasmic fraction from A549 cells after various additions

The changes in SPTLC1, 2, and 3 protein expression in the cytoplasmic extract from A549 cells 4 or 6 h after various additions are shown in Fig. 13. Although the individual addition of DL-PDMP or D-NMAPPD caused a time-dependent increase in SPTLC1, 2, and 3 protein expression compared with the control system, the dual addition did not significantly modify SPTLC1, 2, and 3 protein expression compared with the individual addition. The band of SPTLC1 (56 kDa) may correspond to the phosphorylated isoform of SPTLC1 (53 kDa) [20]. The band of SPTLC3 (35 kDa) may correspond to the splicing isoform missing in isoform 2 (Human Protein Atlas, SPTLC3-201). Neither SPTLC1 (53 and 56 kDa) nor SPTLC2 (63 kDa) in the nuclear extract could be detected, although SPTLC3 (35 kDa) was detected in the nuclear extract on Western blotting (data not shown). It was suggested that the steep increase in d18:0 in the *de novo* synthesis by the dual addition was attributable to factors such as the substrate concentration other than SPTLC1, 2, and 3 protein expression.

4. Discussion

We showed that the dual addition of DL-PDMP (GlcCer inhibitor) and D-NMAPPD (ceramidase inhibitor) to A549 cell culture induced C16:0-Cer accumulation with Cer synthase 5 expression and necrotic cell death with lysosomal rupture with leakage of cathepsin B/alkalization after 2–3 h. This Cer accumulation was followed by a steep increase in d18:0 base levels via the activation of SPT activity by the increase in C16:0-CoA concentration as a substrate after 5–6 h. C16:0-Cer accumulation would likely be caused via the bond of unknown receptors and DL-PDMP and/or D-NMAPPD, followed by CerS5 gene expression (the protein expression). The increase in C16:0-CoA concentration was achieved by activation of the fatty acid synthetic pathway from C2:0-CoA, although the activation mechanisms of the fatty acid synthetic pathway by DL-PDMP and/or D-NMAPPD were unknown. On the other hand, it was observed that the steep increase in d18:0 contents was caused in the optimum C16:0 acid concentration in the culture medium, suggesting the substrate inhibition of SPT activity by C16:0-CoA, that is, a lowering of d18:0 production at the high C16:0 acid concentration. The findings described above are summarized in Fig. 14, although it is unknown in this study whether the necrotic cell death was caused by the lysosomal rupture.

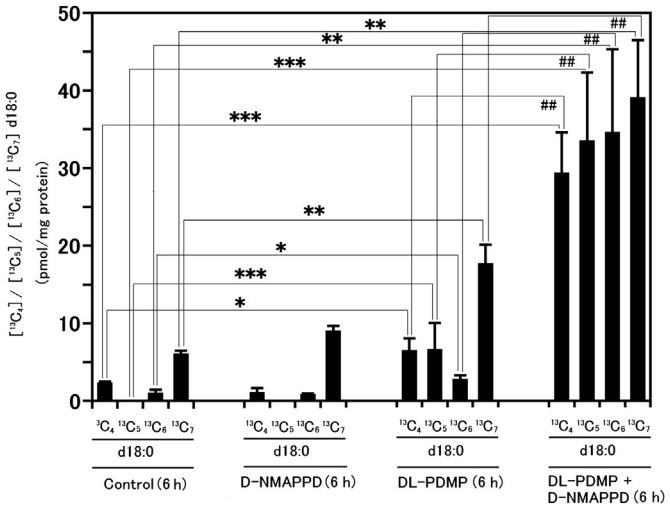

Fig. 10. The dual addition of DL-PDMP and D-NMAPPD caused a significant increase in biosynthesized d18:0 contents via the palmitic acid synthesis pathway from acetic acid. In the tracer experiments, 5.6 mM [2-^{13}C]C2:0 acid in the culture medium was used. The induction of Cer accumulation and extraction/analysis of d18:0 in the homogenate were achieved as described in the Methods. Data are presented as the mean values ± S.D. of three independent experiments; *P < 0.05; **P < 0.01; ***P < 0.001 as compared with the group without the addition. ## indicates P < 0.01 as effects with the dual addition compared with the addition of DL-PDMP.

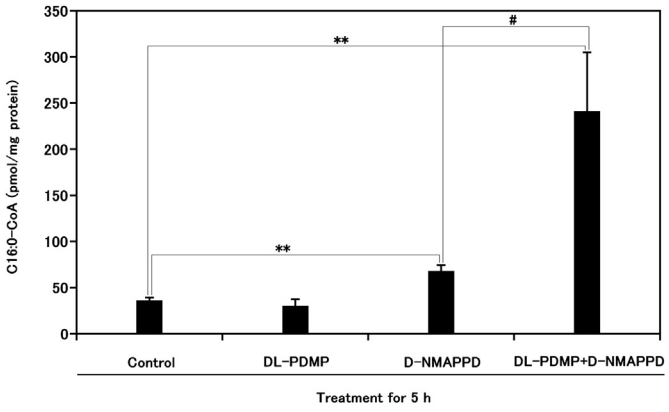

Fig. 11. The dual addition of DL-PDMP and D-NMAPPD caused a significant increase in C16:0-CoA contents. The induction of Cer accumulation and extraction/analysis of C16:0-CoA contents in A549 cells were achieved as described in the Methods. Data are presented as the mean values ± S.D. of three independent experiments; **P < 0.01 as compared with the group without the addition. # indicates P < 0.05 as effects with the dual addition compared with the addition of D-NMAPPD.

These findings suggest a direct link between d18:1-C16:0-Cer/d18:0 biosynthesis and necrotic cell death with the liberation of cathepsin B in A549 cells, which may represent a novel pathway in the cell death mechanism. The slow d18:0/1-deoxysphinganine accumulation in the cells was caused by the addition of fumonisin B(1) as an inhibitor of Cer synthase [21–23] or N-(4-hydroxyphenyl)retinamide (4-HPR) as activators of SPT/alkaline ceramidase 2 and an inhibitor of dihydroceramide desaturase [24,25]. However, the addition of fumonisin B(1) or 4-HPR does not lead to Cer accumulation or a steep increase in SPT activity such as in this study. Therefore, the phenomenon of the increase in d18:1-C16:0-Cer accumulation via the activation of CerS5 and d18:0 base content via the activation of SPT activity may be useful in the analysis of necrotic cell death, lysosomal rupture, CerS5 activity, or SPT activity.

In the protein expressions of CAAT/enhancer binding protein homologous protein (CHOP) as a marker of endoplasmic reticulum stress and microtubule-associated protein 1 light chain 3B (LC3)-II/I as a marker of the autophagosome form using Western blotting as described previously [5], the dual addition did not significantly modify the protein expression compared with the individual addition of 200 μM DL-PDMP or 65 μM D-NMAPPD. However, the individual addition caused an increase in CHOP/LC3II protein expression suggesting the facilitation of autophagy via endoplasmic reticulum stress compared with the control system 4 or 6 h after the addition (data not shown). Furthermore, in the detection of oxidative stress and superoxide using the Total ROS/Superoxide Detection kit (Enzo Life Sciences, Inc.) and fluorescence microscopy 2, 4 or 6 h after the treatment, the dual addition did not significantly modify the fluorescent staining compared with the individual addition (data not shown). It was suggested that necrotic cell death in the dual addition was not caused by excess endoplasmic reticulum stress, the autophagosome form, or oxidant stress. The necrotic cell death in this study accompanies lysosomal rupture based on the liberation of cathepsin B from lysosomes and the inhibition of the autophagosome-lysosome fusion with the increased pH of lysosomes, as shown in Figs. 2, 3 and 14, althoughit remains unknown in this study whether the necrotic cell death was definitively caused by the lysosomal rupture.

In the tracer experiments using [1,2,3,4-$^{13}C_4$]C16:0 acid with the dual addition of DL-PDMP and D-NMAPPD, the variation in the incorporation of ^{13}C into d18:0 via *de novo* synthesis from [1,2,3,4-$^{13}C_4$]C16:0 acid suggests the optimum C16:0 acid concentration in the culture medium, as shown in Fig. 9. The added [1,2,3,4-$^{13}C_4$]C16:0 acid will possibly be transported via FATP1 interacted to acyl coenzyme A synthetase, as described previously [19]. Consequently, the lowered d18:0 production with the incorporation of ^{13}C with a high concentration of C16:0 acid in the culture medium appears to be the result of substrate inhibition by C16:0-CoA as a substrate of SPT activity, as described previously [11]. On the other hand, C16:0 acid at high concentration (500–1250 μM) increases d18:1-1-phosphate independently of *de novo* synthesis via the upregulation of d18:1 kinase [26] or triggers Ca^{2+}-dependent autophagy, which results in programmed necrotic death (necroptosis) of endothelial cells [27]. This information is caused independently of the *de novo* synthesis of Cers, and this tendency is consistent with the phenomenon with a high concentration of C16:0 acid in this study.

In recent years, the formation of Cer channel via the interaction with Bax in the mitochondrial outer membrane, followed by the release of cytochrome c into the cytoplasm in apoptosis and the direct interaction of mitochondrial Cer with the autophagosomal membrane bound-LC3-II in mitophagy have been reported [2,3]. Furthermore, C16:0-Cer directly bound cathepsin D in the lysosomes, and cathepsin D stimulated proteolytic activity, followed by cathepsin D-mediated cleavage of the BH3-only

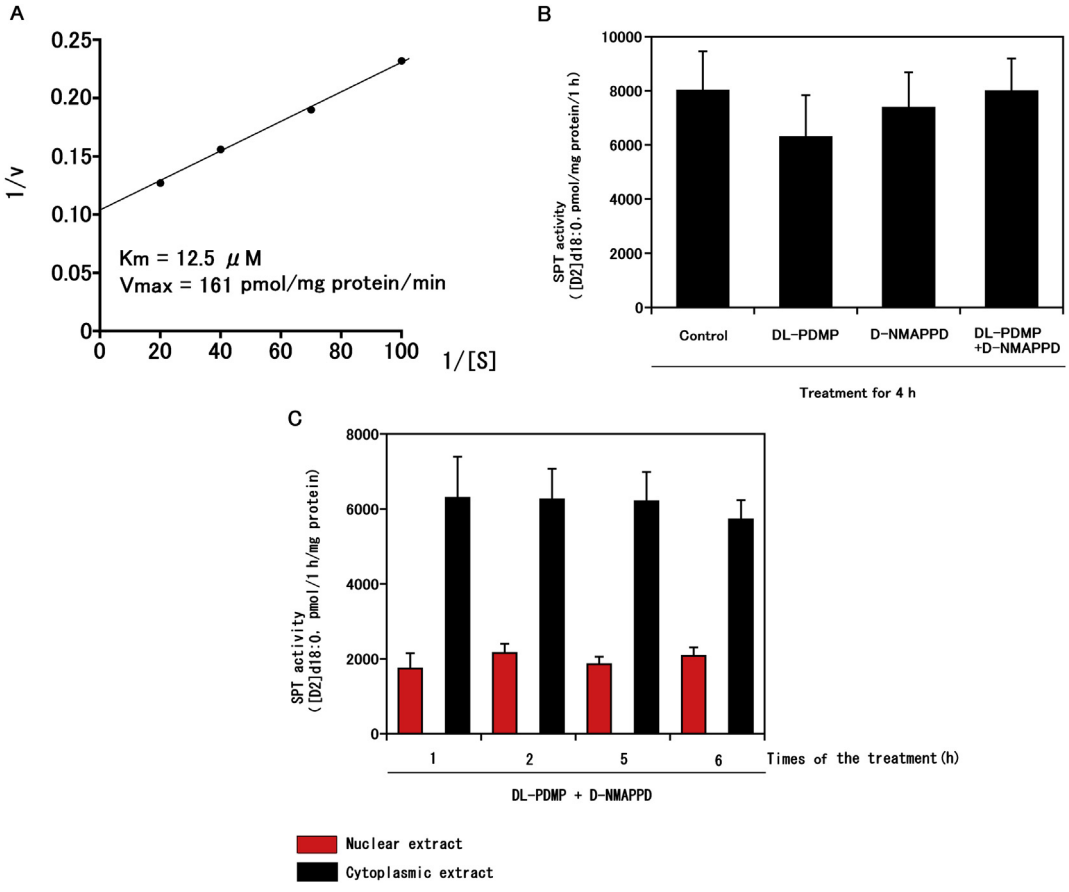

Fig. 12. The dual addition of DL-PDMP and D-NMAPPD to A549 cells did not significantly modify SPT activity in the homogenate or the cytoplasmic or nuclear extract. The induction of Cer accumulation and the measurement of SPT activity/kinetics were achieved as described in the Methods. ***A***, SPT kinetics using the MAM fraction from A549 cells. The *Km* against C16:0-CoA as a substrate was 12.5 μM. The *Vmax* was 161 pmol/mg protein/min. ***B***, SPT activities in the homogenate from A549 cells under various additions. ***C***, Time course of SPT activity of cells in the cytoplasmic or nuclear extract from A549 cells with the dual addition of 200 μM DL-PDMP and 65 μM D-NMAPPD. Data are presented as the mean values ± S.D. of three independent experiments.

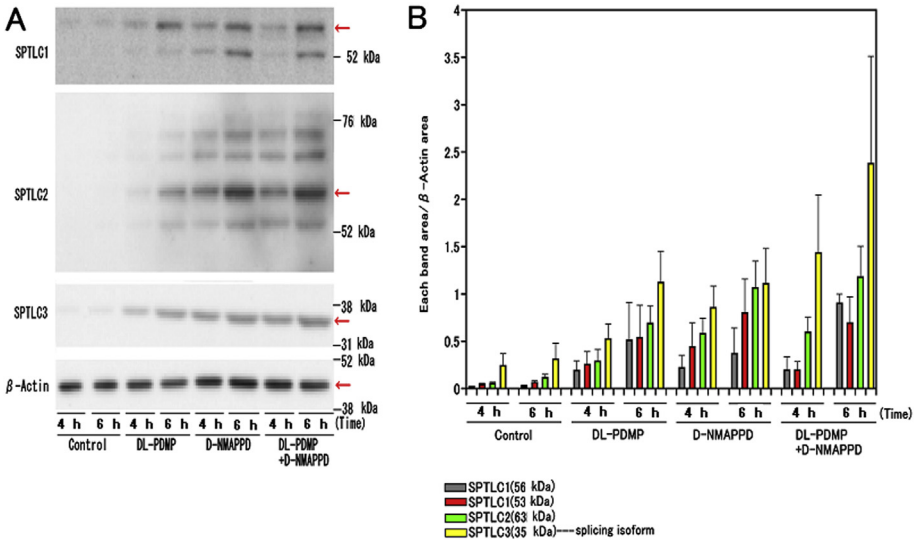

Fig. 13. Although the individual addition of DL-PDMP or D-NMAPPD caused a time-dependent increase in SPTLC1, 2, and 3 protein expression compared with the control system, the dual addition did not significantly modify SPTLC1, 2, and 3 protein expression compared with the individual addition. The induction of Cer accumulation and Western blotting with anti-SPTLC1/2/3 were achieved as described in the Methods. ***A***, Western blot analysis of SPTLC1, 2, 3 and β-actin in the cytoplasmic extract from A549 cells after various additions. The band of SPTLC (56 kDa) may correspond to the phosphorylated isoform of SPTLC1 (53 kDa). The band of SPTLC3 (35 kDa) may correspond to the splicing isoform by the missing isoform 2. ***B***, Changes in each band area/β-actin area ratios related to SPTLC1, 2, and 3 protein expression. Data are presented as the mean values ± S.D. of three independent experiments.

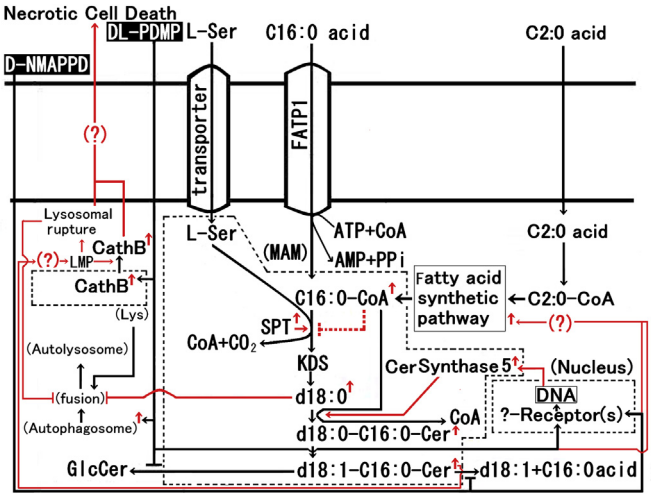

Fig. 14. The dual addition of DL-PDMP (Glc-Cer synthase inhibitor) and D-NMAPPD (ceramidase inhibitor) to the A549 cell culture induced C16:0-Cer accumulation with Cer synthase 5 expression and necrosis with lysosomal rupture with leakage of cathepsin B/alkalization 2–3 h after. This Cer accumulation was followed by a steep increase in the d18:0 base levels via the activation of SPT activity induced by an increase in C16:0-CoA concentration as a substrate 5–6 h after. C16:0-Cer accumulation would likely be caused via the bond of unknown receptors and DL-PDMP and/or D-NMAPPD, followed by CerS5 gene expression (the protein expression). The increase in C16:0-CoA concentration was achieved by activation of the fatty acid synthetic pathway from C2:0-CoA. The activation mechanisms of the fatty acid synthetic pathway by DL-PDMP and/or D-NMAPPD were unknown. Furthermore, it was observed that the steep increase in d18:0 contents was caused in the optimum C16:0 acid concentration in the culture medium, although the high C16:0 acid concentration lowered d18:0 production, suggesting the substrate inhibition of SPT activity by C16:0-CoA. On the other hand, it was stipulated that C16:0-Cer accumulation in lysosomes and the inhibition of lysosomal acid ceramidase by D-NMAPPD were required for the liberation of cathepsin B from lysosomes based on LMP, followed by lysosomal disruption and digestion of vital proteins for a lethal event. It was then stipulated that d18:0 production with the dual addition caused an increase in the pH in acidic compartments such as lysosomes, followed by the inhibition of autophagosome-lysosome fusion.

protein Bid to activate the mitochondrial caspase-dependent pathway of apoptosis, as described previously [28,29]. However, in A549 cells, since active caspase 3 expression with C16:0-Cer accumulation was not detected by the blocking effect in the caspase 9 – 3 process by survivin [4,5], C16:0-Cer accumulation in A549 cells would likely be associated with a pathway (e.g., the pathway of necrotic cell death) other than the mitochondrial caspase-dependent pathway. If C16:0-Cer channels were formed in the lysosome membrane with C16:0-Cer accumulation via the activation of CerS5 and the inhibition of lysosomal acid ceramidase by D-NMAPPD, this possibility is of interest as a function of the liberation of cathepsin B from lysosomes causing necrotic cell death via C16:0-Cer channels other than the mitochondrial caspase-dependent pathway of apoptosis.

The dual addition to the individual addition of DL-PDMP or D-NMAPPD to A549 cells did not significantly modify SPT activity in the homogenate (Fig. 12B) or STPLC1, 2, and 3 protein expression in the cytoplasmic extract (Fig. 13), although the individual addition or the dual addition caused an increase in SPTLC1, 2, and 3 protein expression compared with the control system. Eukaryotic SPTs are membrane-bound multisubunit enzymes and the functional SPT is not a dimer, but a higher organized complex composed of three distinct subunits with a molecular mass of 480 kDa [30]. Furthermore, the small subunits of human SPT activating the heterodimer have been recently found [31]. Although the function of a higher organized complex from SPTLC1, 2, and 3 proteins or the small subunits of human SPT in this study is not clear, the steep increase in d18:0 *de novo* synthesis with the dual addition is likely caused by factors such as the substrate (C16:0-CoA) concentration as shown in Figs. 10 and 11 other than the SPT enzyme (SPTLC1, 2, 3 and the small subunits) concentration. The steep increase in d18:0 content possibly caused an increase in the pH in acidic compartments such as lysosomes, followed by the inhibition of the increased autophagosome-lysosome fusion, lysosomal rupture, and necrotic cell death [14,16].

D-NMAPPD at 50 μM exhibited an inhibitory effect on acid ceramidase and cell growth, although neither the acid ceramidase expression nor lysosomal stability could be altered [32]. Thus, D-NMAPPD is an acid ceramidase inhibitor, not a lysosomal trapping drug. On the other hand, DL-PDMP as an inhibitor of Glc-Cer synthase exhibited an inhibitory effect on cell growth via the inhibition of protein/DNA synthesis although this drug acts as a lipophilic amine/lysosomal trapping drug at high concentrations, and the effect is observed 24 h after the addition in culture cells [33]. However, its effects as a lysosomal trapping drug of DL-PDMP are not observed 3 h after the addition, as described in Fig. 3C. Thus, the lysosomal effects of the dual addition of DL-PDMP and D-NMAPPD are likely caused by the mechanism shown in Fig. 14.

5. Conclusions

The aim of this study was to examine the relationship between Cer accumulation with inhibition of the conversion pathway of Cer and concomitant necrotic cell death. As active caspase 3 expression with C16:0-Cer accumulation in A549 cells was not detected by the inhibiting effect of caspase 9 activation brought about by survivin in the cells, Cer accumulation in A549 cells would likely be associated with a pathway other than the mitochondrial caspase-dependent pathway of apoptosis. We showed that the dual addition of DL-PDMP (GlcCer synthase inhibitor) and D-NMAPPD (ceramidase inhibitor) to A549 cell culture induced C16:0-Cer accumulation with CerS5 expression and necrotic cell death with lysosomal rupture and with leakage of cathepsin B/alkalization after 2–3 h. This Cer accumulation was followed by a steep increase in d18:0 base levels via the activation of SPT activity brought about by the increase in C16:0-CoA concentration as a substrate after 5–6 h. The increase in C16:0-CoA concentration was achieved by activation of the fatty acid synthetic pathway from C2:0-CoA. Furthermore, it was observed that the steep increase in d18:0 contents was caused at the optimum C16:0 acid concentration in the culture medium, suggesting the substrate inhibition of SPT activity

by C16:0-CoA, that is, a lowering of d18:0 production at the high C16:0 acid concentration.

Conflict of interest

The corresponding author (Mototeru Yamane) has no conflict of interest associated with this study.

Acknowledgments

I thank Dr. S. Moriya for the acquisition of Western blot data related to CHOP/LC3BII/p62 expression and for help with the graphic work. I am also indebted to Dr. Edward Barroga, Senior Editor of the Department of International Medical Communications of Tokyo Medical University for editing the manuscript.

References

[1] S. Schiffmann, K. Birod, J. Männich, M. Eberle, M.-S. Wegner, R. Wanger, D. Hartmann, N. Ferreiros, G. Geisslinger, S. Grösch, Ceramide metabolism in mouse tissue, Int. J. Biochem. Cell Biol. 45 (2013) 1886–1894.

[2] M. Colombini, Membrane channels formed by ceramide, Handb. Exp. Pharmacol. 215 (2013) 109–126.

[3] R.D. Sentelle, C.E. Senkal, W. Jiang, S. Ponnusamy, S. Gencer, S.P. Selvam, V.K. Ramshesh, Y.K. Peterson, J.J. Lemasters, Z.M. Szulc, J. Bielawski, B. Ogretman, Ceramide targets autophagosomes to mitochondria and induces lethal mitophagy, Nat. Chem. Biol. 8 (2012) 831–838.

[4] A. Ogura, Y. Watanabe, D. Iizuka, H. Yasui, M. Amitani, S. Kobayashi, M. Kuwabara, O. Inanami, Radiation-induced apoptosis of tumor cells is facilitated by inhibition of the interaction between Survivin and Smac/DIABLO, Cancer Lett. 259 (2008) 71–81.

[5] M. Yamane, K. Miyazawa, S. Moriya, A. Abe, S. Yamane, D,L-Threo-1-phenyl-2-decanoylamino-3-morpholino-1-propanol (DL-PDMP) increases endoplasmic reticulum stress, autophagy and apoptosis accompanying ceramide accumulation via ceramide synthase 5 protein expression in A549 cells, Biochimie 93 (2011) 1446–1459.

[6] J. Inokuchi, N.S. Radin, Metabolism of D-[3H]threo-1-phenyl-2-decanoylamino-3-morpholino-1-propanol, an inhibitor of glucosylceramide synthesis, and the synergistic action of an inhibitor of microsomal monooxygenase, J. Lipid Res. 28 (1987) 565–571.

[7] M. Selzner, A. Bielawska, M. Morse, H.A. Rüdiger, D. Sindram, Y.A. Hannun, P.-A. Clavien, Induction of apoptotic cell death and prevention of tumor growth by ceramide analogues in metastatic human colon cancer, Cancer Res. 61 (2001) 1233–1240.

[8] A.A. Spector, J.C. Hoak, An improved method for the addition of long-chain free fatty acid to protein solutions, Anal. Biochem. 32 (1969) 297–302.

[9] D. Sun, M.G. Cree, R.R. Wolfe, Quantification of the concentration and 13C tracer enrichment of long-chain fatty acyl-coenzyme A in muscle by liquid chromatography/mass spectrometry, Anal. Biochem. 349 (2006) 87–95.

[10] A.U. Blachnio-Zabielska, C. Koutsari, M.D. Jensen, Measuring long-chain acyl-coenzyme A concentrations and enrichment using liquid chromatography/tandem mass spectrometry with selected reaction monitoring, Rapid Commun. Mass Spectrom. 25 (2011) 2223–2230.

[11] M.F. Rütti, S. Richard, A. Penno, A. Eckardstein, T. Hornemann, An improved method to determine serine palmitoyltransferase activity, J. Lipid Res. 50 (2009) 1237–1244.

[12] Y. Shiraiwa, H. Ikushiro, H. Hayashi, Multifunctional role of His159in the catalytic reaction of serine palmitoyltransferase, J. Biol. Chem. 284 (2009) 15487–15495.

[13] B.F. Howell, S. McCune, R. Schaffer, Lactate-to-pyruvate or pyruvate-to-lactate assay for lactate dehydrogenase: a re-examination, Clin. Chem. 25 (1979) 269–272.

[14] K. Kagedal, M. Zhao, I. Svensson, U.T. Brunk, Sphingosine-induced apoptosis is dependent on lysosomal proteases, Biochem. J. 359 (2001) 335–343.

[15] K.E. Choi, Y.S. Jung, D.H. Kim, J.K. Song, J.Y. Kim, Y.Y. Jung, S.Y. Eum, J.H. Kim, N.Y. Yoon, H.S. Yoo, S.B. Han, J.T. Hong, Myriocin induces apoptotic lung cancer cell death via activation of DR4 pathway, Arch. Pharm. Res. 37 (2014) 501–511.

[16] A. Kawai, H. Uchiyama, S. Takano, N. Nakamura, S. Ohkuma, Autophagosome-lysosome fusion depends on the pH in acidic compartments in CHO cells, Autophagy 3 (2007) 154–157.

[17] S.F. Meng, W.P. Mao, F. Wang, X.Q. Liu, L.L. Shao, The relationship between Cd-induced autophagy and lysosomal activation in WRL-68 cells, J. Appl. Toxicol. (2015). http://dx.doi.org/10.1002/jat.3114.

[18] A.M. Hall, A.J. Smith, D.A. Bernlohr, Characterization of the Acyl-CoA synthetase activity of purified murine fatty acid transport protein 1, J. Biol. Chem. 278 (2003) 43008–43013.

[19] M.R. Richards, J.D. Harp, J.D.S. Ory, J.E. Schaffer, Fatty acid transport protein 1 and long-chain acyl coenzyme A synthetase 1 interact in adipocytes, J. Lipid Res. 47 (2006) 665–672.

[20] S. Taouji, A. Higa, F. Delom, S. Palcy, F.-X. Mahon, J.-M. Pasquet, R. Bossé, B. Ségul, E. Chevet, Phosphorylation of serine palmitoyltransferase long chain-1 (SPTLC1) on tyrosine 164 inhibits its activity and promotes cell survival, J. Biol. Chem. 288 (2013) 17190–17201.

[21] E.M. Schmelz, M.A. Dombrink-Kurtzman, P.C. Roberts, Y. Kozutsumi, T. Kawasaki, A.H. Merrill Jr., Induction of apoptosis by fumonisin B1 in HT29 cells is mediated by the accumulation of endogenous free sphingoid bases, Toxicol. Appl. Pharmacol. 148 (1998) 252–260.

[22] M.F. Osuchowski, R.P. Sharma, Fumonisin B1 induces necrotic cell death in BV-2 cells and murine cultured astrocytes and is antiproliferative in BV-2 cells while N2A cells and primary cortical neurons are resistant, Neurotoxicology 26 (2005) 981–992.

[23] N.C. Zitomer, T. Mitchell, K.A. Voss, G.S. Bondy, S.T. Pruett, E.C. Garnier-Amblard, L.S. Liebeskind, H. Park, E. Wang, M.C. Sullards, A.H. Merrill Jr., R.T. Riley, Ceramide synthase inhibition by fumonisin B1 causes accumulation of 1-deoxysphinganine: a novel category of bioactive 1-deoxysphingoid bases and 1-deoxydihydroceramides biosynthesized by mammalian cell lines and animals, J. Biol. Chem. 284 (2009) 4786–4795.

[24] H. Wang, B.J. Maurer, Y.-Y. Liu, E. Wang, J.C. Allegood, S. Kelly, H. Symolon, Y. Liu, A.H. Merrill Jr., V. Gouazé-Andersson, J.Y. Yu, A.E. Giuliano, M.C. Cabot, N-(4-Hydroxyphenyl)retinamide increases dihydroceramide and synergizes with dimethylsphingosine to enhance cancer cell killing, Mol. Cancer Ther. 7 (2008) 2967–2976.

[25] Z. Mao, W. Sun, R. Xu, S. Novgorodov, Z.M. Szulc, Z.J. Bielawski, L.M. Obeid, C. Mao, Alkaline ceramidase 2 (ACER2) and its product dihydrosphingosine mediate the cytotoxicity of N-(4-hydroxyphenyl)retinamide in tumor cells, J. Biol. Chem. 285 (2010) 29078–29090.

[26] W. Hu, J. Bielawski, F. Samad, A.H. Merrill Jr., L.A. Cowart, Palmitate increases sphingosine-1-phosphate in C2C12 myotubes via upregulation of sphingosine kinase message and activity, J. Lipid Res. 50 (2009) 1852–1862.

[27] M.J. Khan, M.R. Alam, M. Waldeck-Weiermair, F. Karsten, L. Groschner, M. Riederer, S. Hallström, P. Rockenfeller, V. Konya, A. Heinemann, F. Madeo, W.F. Graier, R. Malli, Inhibition of autophagy rescues palmitic acid-induced necroptosis of endothelial cells, J. Biol. Chem. 287 (2012) 21110–21120.

[28] M. Heinrich, M. Wickel, W. Schneider-Brachert, C. Sandberg, J. Gahr, R. Schwandner, T. Weber, J. Brunner, M. Krönke, S. Schütze, Cathepsin D targeted by acid sphingomyelinase-derived ceramide, EMBO J. 18 (1999) 5252–5263.

[29] C.A. Dumitru, I.E. Sandalcioglu, M. Wagner, M. Weller, E. Gulbins, Lysosomal ceramide mediates gemcitabine-induced death of glioma cells, J. Mol. Med. (Berl.) 87 (2009) 1123–1132.

[30] T. Hornemann, Y. Wei, A.V. Eckardstein, Is the mammalian serine palmitoyltransferase a high-molecular-mass complex? Biochem. J. 405 (2007) 157–164.

[31] J.M. Harmon, D. Bacikova, K. Gable, S.D. Gupta, G. Han, N. Sengupta, T.M. Dunn, Topological and functional characterization of the ssSPTs, small activating subunits of serine palmitoyltransferase, J. Biol. Chem. 288 (2013) 10144–10153.

[32] A. Bai, Z.M. Szulc, J. Bielawski, N. Mayroo, X. Liu, J. Norris, Y.A. Hannun, A. Bielawska, Synthesis and bioevaluation of omega-N-amino analogs of B13, Bioorg. Med. Chem. 17 (2009) 1840–1848.

[33] A.G. Rosenwald, R.E. Pagano, Effects of the glucosphingolipid synthesis inhibitor, PDMP, on lysosomes in cultured cells, J. Lipid Res. 35 (1994) 1232–1240.